Dr Bright.

DEPARTMENT OF
ENERGY, MINES AND RESOURCES
MINES BRANCH
OTTAWA

AN INTRODUCTION TO THE THEORY, MEASUREMENT AND APPLICATION OF SEMICONDUCTOR TRANSPORT PROPERTIES OF MINERALS

T. M. BALESHTA AND H. P. DIBBS

MINERAL SCIENCES DIVISION

JANUARY 1969

Technical Bulletin TB 106 Price $1.00

© Crown Copyrights reserved

Available by mail from the Queen's Printer, Ottawa,
and at the following Canadian Government bookshops:

HALIFAX
1735 Barrington Street

MONTREAL
Æterna-Vie Building, 1182 St. Catherine St. West

OTTAWA
Daly Building, Corner Mackenzie and Rideau

TORONTO
221 Yonge Street

WINNIPEG
Mall Center Bldg., 499 Portage Avenue

VANCOUVER
657 Granville Street

or through your bookseller

Price $1.00 Catalogue No. M34-20-106

Price subject to change without notice

ROGER DUHAMEL, F.R.S.C.
Queen's Printer and Controller of Stationery
Ottawa, Canada
1968

Mines Branch Technical Bulletin TB 106

AN INTRODUCTION TO THE THEORY, MEASUREMENT AND APPLICATION OF SEMICONDUCTOR TRANSPORT PROPERTIES OF MINERALS

by

T. M. Baleshta* and H. P. Dibbs**

- - -

ABSTRACT

An introductory account is given of some of the basic ideas of semiconductor physics and of the measurement techniques frequently used to characterize semiconductor transport behaviour. The application of some of these ideas and measurements to mineral beneficiation is discussed.

*Research Scientist and **Head, Surface Science Group; Mineral Sciences Division, Mines Branch, Department of Energy, Mines and Resources, Ottawa, Canada.

Bulletin technique TB 106

Direction des mines

UNE INTRODUCTION À LA THÉORIE, LA MESURE ET L'APPLICATION DES PROPRIÉTÉS SEMICONDUCTRICES DES MINÉRAUX

par

T.M. Baleshta* et H. P. Dibbs**

RÉSUMÉ

Cette étude comporte un exposé préliminaire de certains concepts de base de la physique des semi-conducteurs et des méthodes de mesure généralement utilisées pour caractériser les propriétés semiconductrices de certains minéraux. Les auteurs traitent également de l'application de certains de ces concepts et méthodes de mesure à l'enrichissement des minéraux.

* Chercheur scientifique et ** chef, Groupe des sciences de la surface, Division des sciences minérales, Direction des mines, ministère de l'Énergie, des Mines et des Ressources, Ottawa, Canada.

CONTENTS

	Page
Abstract	i
Resumé	ii
Introduction	1
The Energy-Band Model of Semiconductors	2
(a) Intrinsic Semiconductor	2
(b) n-Type Semiconductor	3
(c) p-Type Semiconductor	6
The Measurement of Semiconductor Properties	10
The Problem of Ohmic Contacts	10
Bulk Property Measurements	11
1. Conductivity	11
2. Carrier Mobility	13
3. Fermi Energy and Activation Energy	16
4. Thermoelectric Power	19
Energy Barrier Measurements	20
1. Semiconductor-Metal Contact	20
2. Semiconductor-Electrolyte Interface	31
Surface Property Measurements	33
Some Applications of Semiconductor Principles	34
References	38
<u>Appendix 1</u> - Band-Gap Energies of Mineral-Type Semiconductors (Sulphides)	40
<u>Appendix 2</u> - Typical Transport Measurement Data on Mineral-Type Semiconductors (Sulphides)	41-60

= = =

FIGURES

No.		Page
1.	Energy-band model for an intrinsic semiconductor.. ..	4
2.	Energy-band model for an n-type (extrinsic) semiconductor	5
3.	Energy-band model for a p-type (extrinsic) semiconductor	8
4.	Energy-band diagram showing the potential change between the surface and bulk of an intrinsic semiconductor	9
5.	Energy-band diagram for an ohmic contact to an n-type semiconductor	12
6.	Energy-band diagram for an ohmic contact to a p-type semiconductor	12
7.	A diagrammatic view of the effect of a magnetic field on positive charge carriers in a crystal	14
8.	Fermi-energy level versus temperature for a typical n-type semiconductor	17
9.	Intrinsic and extrinsic carrier concentration versus temperature of a typical n-type semiconductor	18
10.	Schematic structure and energy-level diagram of a typical n-type semiconductor/metal interface ..	22
11.	Variation of $^{1}/_{C^2}$ versus bias voltage CdS/Au interface (after Goodman, A., ref. 30-31)	23
12.	Energy-band diagram for an n-type semiconductor/metal interface where	24
13.	Energy-band diagram for a p-type semiconductor/metal interface where	25
14.	Energy-band diagram for an n-type semiconductor where	26
15.	Energy-band diagram for a p-type semiconductor/metal interface where	27
16.	Voltage-current characteristic of a p-type PbS/Al contact at 77°K	29

(Figures, cont'd) -

No.		Page
17.	Log J versus bias voltage of a PbS/Al interface	30
18.	Structure of the double layer (a), potential distribution (b) and equivalent circuit (c), at the semiconductor-electrolyte interface	32
19.	Resistivity versus reciprocal temperature of n-type arsenopyrite	(In Appendix 2) 42
20.	Thermoelectric power versus temperature of the arsenopyrite sample in Figure 19	43
21.	Resistivity versus reciprocal temperature of p-type bornite	44
22.	Thermoelectric power versus reciprocal temperature of the bornite sample in Figure 21	45
23.	Resistivity versus reciprocal temperature of n-type chalcopyrite	46
24.	Thermoelectric power versus temperature of the chalcopyrite sample in Figure 23	47
25.	Resistivity versus reciprocal temperature of p-type digenite	48
26.	Thermoelectric power versus temperature of the digenite sample in Figure 25	49
27.	Conductivity versus reciprocal temperature of synthetic galena, p-type	50
28.	Hole mobility versus reciprocal temperature of the galena sample in Figure 27	51
29.	Resistivity versus reciprocal temperature of p-type marcasite	52
30.	Thermoelectric power versus temperature of the marcasite sample in Figure 29	53
31.	Conductivity versus reciprocal temperature of a variety of n-type pyrite samples	54
32.	Thermoelectric power versus temperature of the n-type pyrite samples in Figure 31	55
33.	Mobility versus reciprocal temperature of the pyrite samples in Figure 31	56

(Figures, concluded)

No.		Page
34.	Resistivity versus reciprocal temperature of two p-type pyrrhotite samples	57
35.	Thermoelectric power versus temperature of the pyrrhotite samples in Figure 34	58
36.	Conductivity versus reciprocal temperature of zinc sulphide-16 wt % iron doped (p-type)	59
37.	Thermoelectric power versus temperature of the zinc sulphide sample in Figure 36	60

TABLE

1.	Band-Gap Energies of Mineral-Type Semiconductors (Sulphides)	40
		(In Appendix 1)

= = =

INTRODUCTION

A good understanding exists of the properties of elemental semiconductors, and of the marked effects that are produced on their electrical, thermal and surface properties by the deliberate addition of very small amounts of impurities. Since many naturally occurring minerals of economic importance are semiconductors (e.g. chalcopyrite, galena, pyrite), it is important to consider the possible applications of the concepts of solid-state physics to these minerals, with the object of gaining a better understanding of mineral behaviour in beneficiation processes, and also to consider the possibility of improving this behaviour by surface pretreatment of the minerals. However, many people who are concerned with mineral investigation may be unfamiliar with solid-state physics and thus hampered in the application of some of the more elementary, but nevertheless far-reaching, concepts involved. For example, some early attempts to classify minerals on the basis of their electrical conductivities were not very successful (1), primarily through a lack of understanding, at that time, of the basic physics of the property being measured (2).

It is the purpose of this report to give an elementary introduction to some of the more important theoretical concepts that are used in semiconductor physics, and also to give a description of the more frequently measured electrical transport properties characteristic of semiconductors. Some typical experimental data are included in Appendices 1 and 2, to provide a "feeling" for the units and numerical values involved in these measurements.

A number of standard formulae will be quoted in this report. No attempt has been made to prove these formulae, but literature references are provided for further reading if desired. Finally, the application to practical systems of some of the ideas presented will be outlined, with particular reference to mineral separation.

THE ENERGY-BAND MODEL OF SEMICONDUCTORS

The bulk energy structure of a semiconductor is conventionally represented by an energy-band diagram. This diagram is derived from quantum-mechanical considerations of the electron energy distribution in a crystal which results when an assemblage of initially isolated atoms is brought together to form a solid phase (3). The model consists of a valence band (energy, E_V) and a conduction band (energy, E_C), separated by a forbidden energy-region -- the band gap (energy, E_G). With the application of Fermi-Dirac statistics, this model shows how impurities (or stoichiometric deviations in a compound semiconductor), temperature, and band-gap energy affect the number of charge carriers that are available in the solid for transport.

A summary will be given, below, of three well-defined situations arising from the energy-band approach; namely, the intrinsic, n-type and p-type semiconductors.

(a) Intrinsic Semiconductor

Figure 1 shows the relative energy states for electrons in a pure or intrinsic semiconductor, i.e. a semiconductor that does not contain any impurities. An increase in temperature (thermal energy) will cause some electrons from the valence band to be redistributed into the conduction band by jumping the band gap. This process gives rise to additional crystal conduction. The electron vacancies, or holes, left in the valence band, may be regarded as positive-charge carriers (concentration, p_i/cm^3) and are equal in number to the negative-charge carriers (electrons; concentration, n_i/cm^3) in the conduction band. At a given temperature, the intrinsic charge-carrier product, $n_i p_i$, is a constant, and relates to the maximum number of charge carriers in the crystal, which is $n_i + p_i$.

The occupation of energy states in the valence band and in the conduction band is a function of the number of available states and the thermal excitation of charge carriers into these states. The thermal redistribution of charge carriers is statistical and obeys the Fermi-Dirac distribution law. This distribution law is analogous to Maxwell-Boltzman statistics used in the description of classical transport behaviour.

The number of intrinsic charge carriers can be calculated from the relation (4) below:

$$n_i = p_i = \sqrt{N_C N_V} \cdot \frac{1}{1 + \exp\left(\frac{E_C - E_V}{2kT}\right)}, \quad \ldots \quad \text{(Eq. 1)}$$

where

$$N_C = 2(2\pi m_e^* kT/h^2)^{\frac{3}{2}} \quad \ldots \quad \text{(Eq. 2)}$$

is the number of available electron energy states in the conduction band, and

$$N_V = 2(2\pi m_p^* kT/h^2)^{\frac{3}{2}} \quad \ldots \quad \text{(Eq. 3)}$$

is the number of unoccupied electron states in the valence band. Equations 2 and 3 show that N_C and N_V are directly related to each other by the values of the effective masses for electrons, m_e^*, and for holes, m_p^*. The distribution of charge carriers in a semiconductor is statistical, and the term containing the exponential in Equation 1 is a probability factor. It can be shown (4-6) that, at any temperature above 0°K, the probability factor is always one-half of the energy between the occupied states and the depopulated states. For intrinsic material the probability factor, E_F, is $\frac{E_C - E_V}{2}$, where E_F is the Fermi energy.

(b) n-Type Semiconductor

Figure 2 shows the relative energy states for electrons in an n-type semiconductor, i.e., a semiconductor containing a donor impurity level close to the conduction band. The donor impurity atoms give up their electrons much more readily than the host atoms, because of the smaller energy gap for the impurity-atom electrons, $E_C - E_D$, as compared with

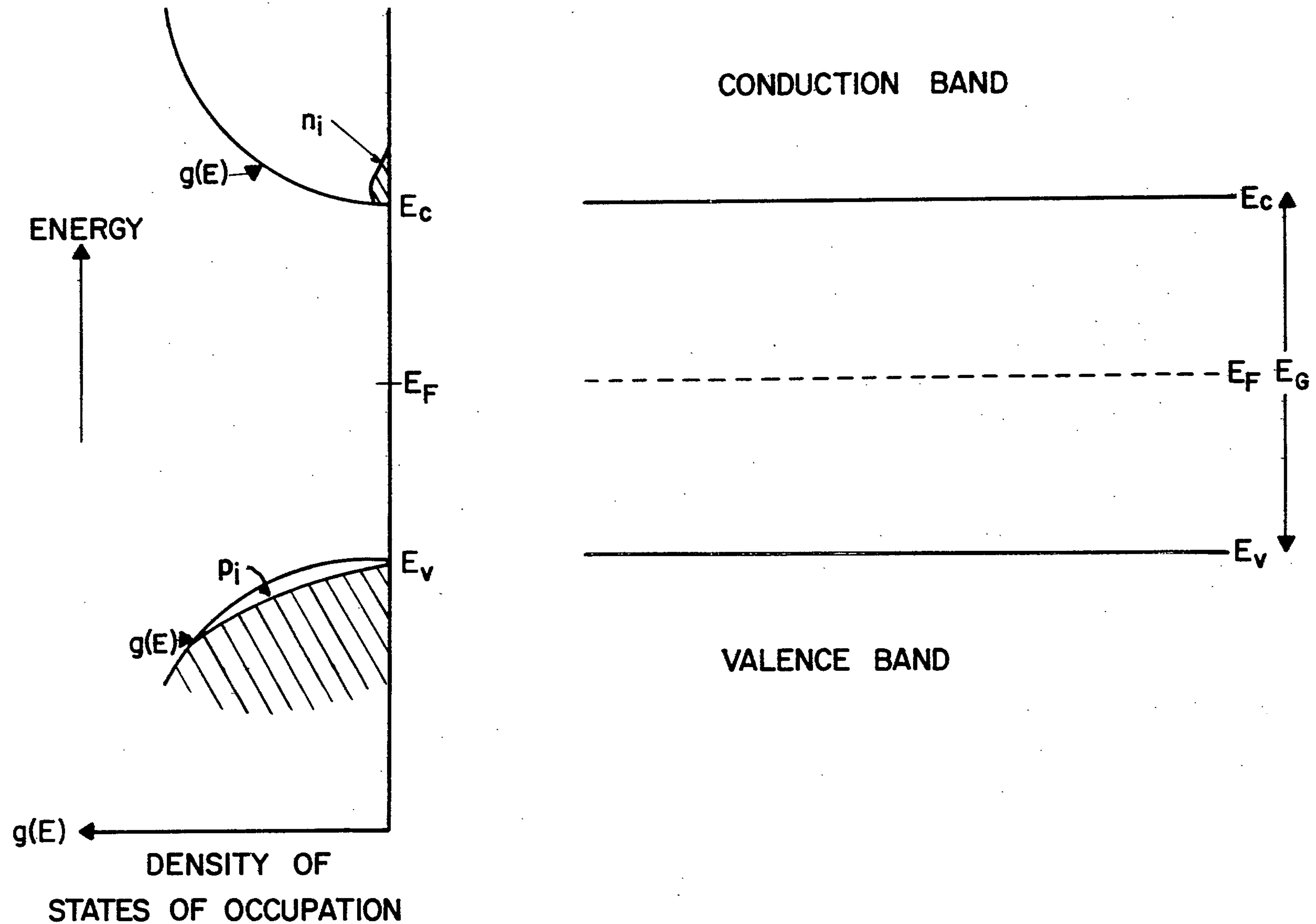

FIGURE 1. Energy-band model for an intrinsic semiconductor. The shaded areas represent occupied energy states.

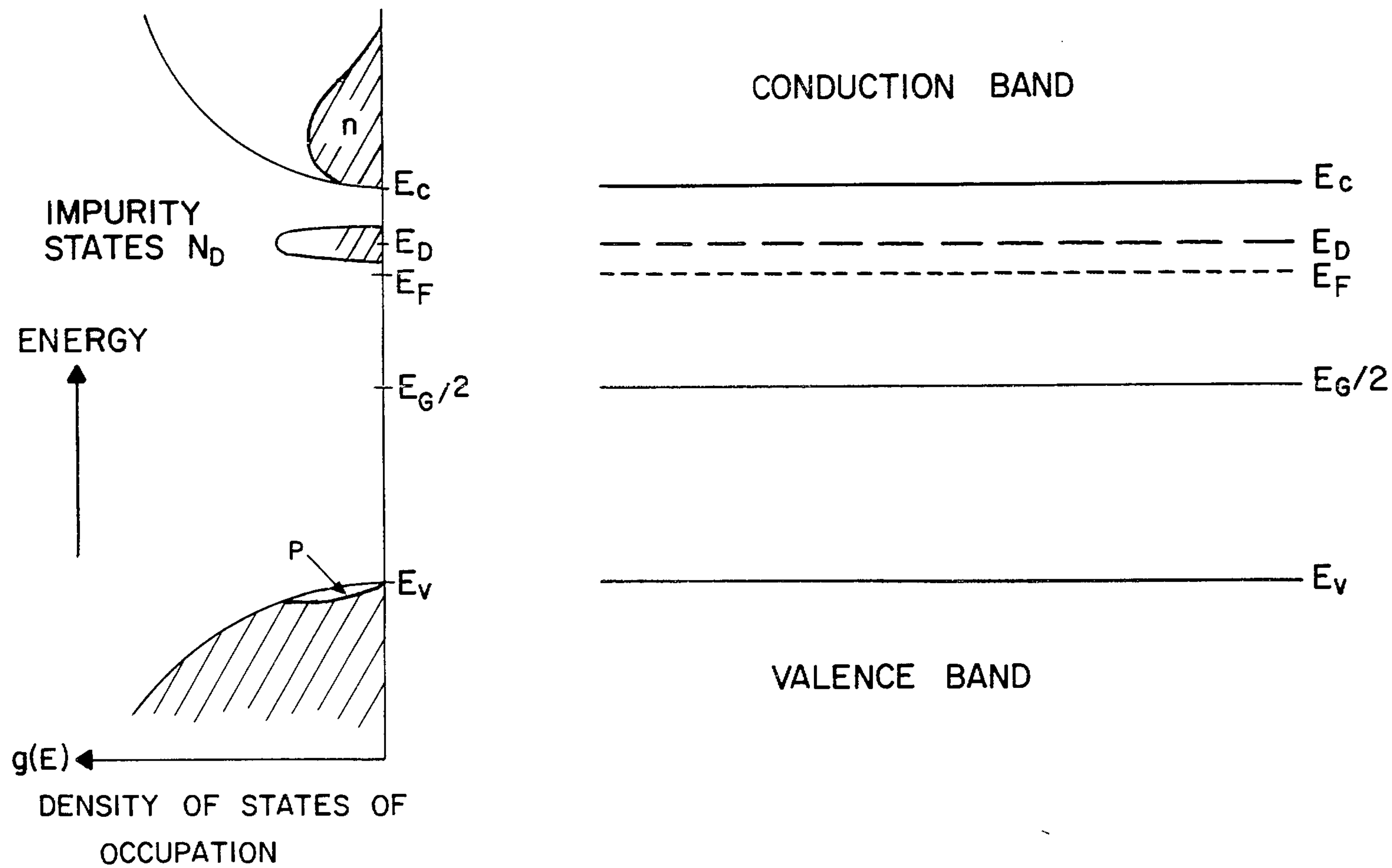

FIGURE 2. Energy-band model for an n-type (extrinsic) semiconductor.

$E_C - E_V$ for electrons from the host atoms. Compared with an intrinsic semiconductor, the majority of charge carriers in an n-type semiconductor are electrons, i.e. $n \gg p$, and electrical neutrality is maintained by the ionized donor atoms. The number of electrons in the conduction band is given by the relation (4-6):

$$n = N_C \cdot \frac{1}{1 + \exp\left(\frac{E_C - E_F}{kT}\right)} \quad \ldots \quad \text{(Eq. 4)}$$

(c) p-Type Semiconductor

The energy-band diagram for a p-type semiconductor is shown in Figure 3 and is analogous to the diagram for an n-type semiconductor, except that an electron acceptor level is located close to the valence band and acts as an electron trap. The majority current carriers in this case are holes, i.e. $p \gg n$, and the number of holes in the valence band is given by (4-6):

$$p = N_V \cdot \frac{1}{1 + \exp\left(\frac{E_F - E_V}{kT}\right)} \quad \ldots \quad \text{(Eq. 5)}$$

The Fermi-Dirac distribution law applies to both n-type and p-type semiconductors, but its application is somewhat more complicated in these cases than in the intrinsic case (3-6), since the position of the Fermi level (E_F) in the forbidden region is dependent both on the temperature and on the impurity concentration. This will be considered later with regard to Fermi level determinations (page 16). However, for all three materials, at a given temperature, the general relation holds that

$$np = \text{constant} = n_i p_i \quad \ldots \quad \text{(Eq. 6)}$$

which is analogous to the ionic product of water where $[H^+][OH^-] = K_W$.

The Fermi level is an extremely important parameter in solid-state physics, and has particular implications whenever two phases or two materials are in equilibrium. It may be shown, by thermodynamic arguments (7), that the Fermi level represents the chemical potential (or average

energy) of an electron in the semiconductor. Thus, the work function of a material is the energy required to take an electron from the Fermi level and place it just outside the material. Since the position of the Fermi level in doped material is dependent both on the temperature and on the impurity content, some control over the thermodynamic properties of electrons is available.

While the bulk behaviour of the charge carriers in a semiconductor (energy or potential) may be described as above, in practice two lattice potentials exist in a semiconductor and the charge carriers will be affected by these potentials. One potential arises from the bulk atoms, while the second potential is from atoms in the surface region. The difference in lattice potentials is the result of surface states (known as Tamm states or Schockley states, depending on the model used) that arise because the surface atoms are bonded in a different manner than the bulk atoms (7-10). The change in potential at the surface acts as a restoring force to maintain charge equilibrium. In addition, other surface states may exist, because of local defects or from absorbed impurities, such as oxygen. The effects described above create two charge-carrier environments, one at the surface and the other in the bulk of the semiconductor, that are separated by a space-charge region. Because the bulk and surface energy states are in thermal equilibrium, they share a common Fermi energy. Energy differences, such as the space-charge potential, are shown as macroscopic energy-band shifts relative to the Fermi level. An energy-band diagram showing the band shift in the surface region of an intrinsic semiconductor is given in Figure 4.

Characterization of the surface region can be made from <u>bulk</u> properties when the space-charge potential is known. Bulk properties are obtained from volume-type measurements such as conductivity. The space-charge potential is obtained by combining the charge-carrier concentration in the bulk and the space-charge capacitance. Surface parameters can also be directly measured by field effect (11-13) or by optical methods (11, 14).

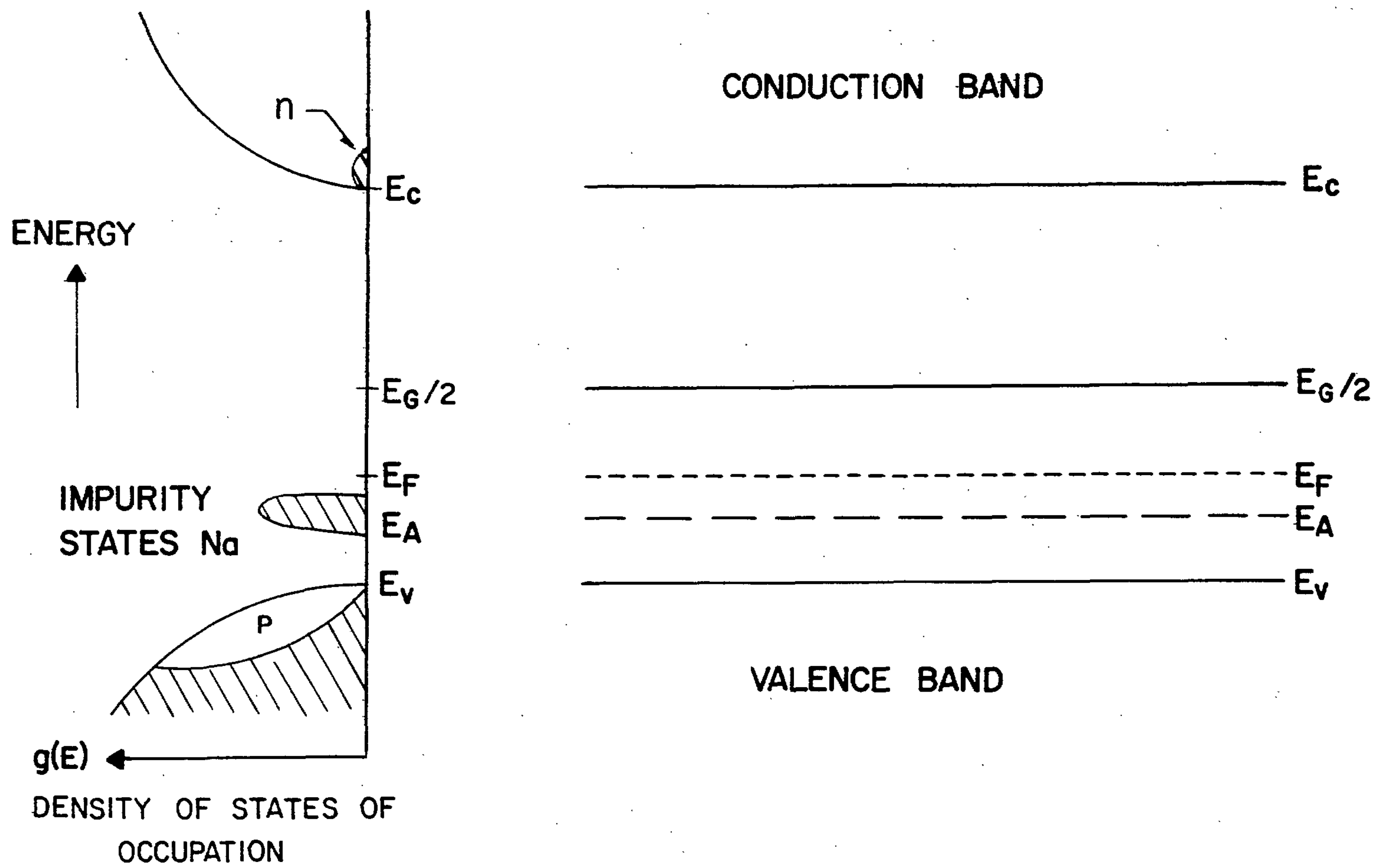

FIGURE 3. Energy-band model for a p-type (extrinsic) semiconductor.

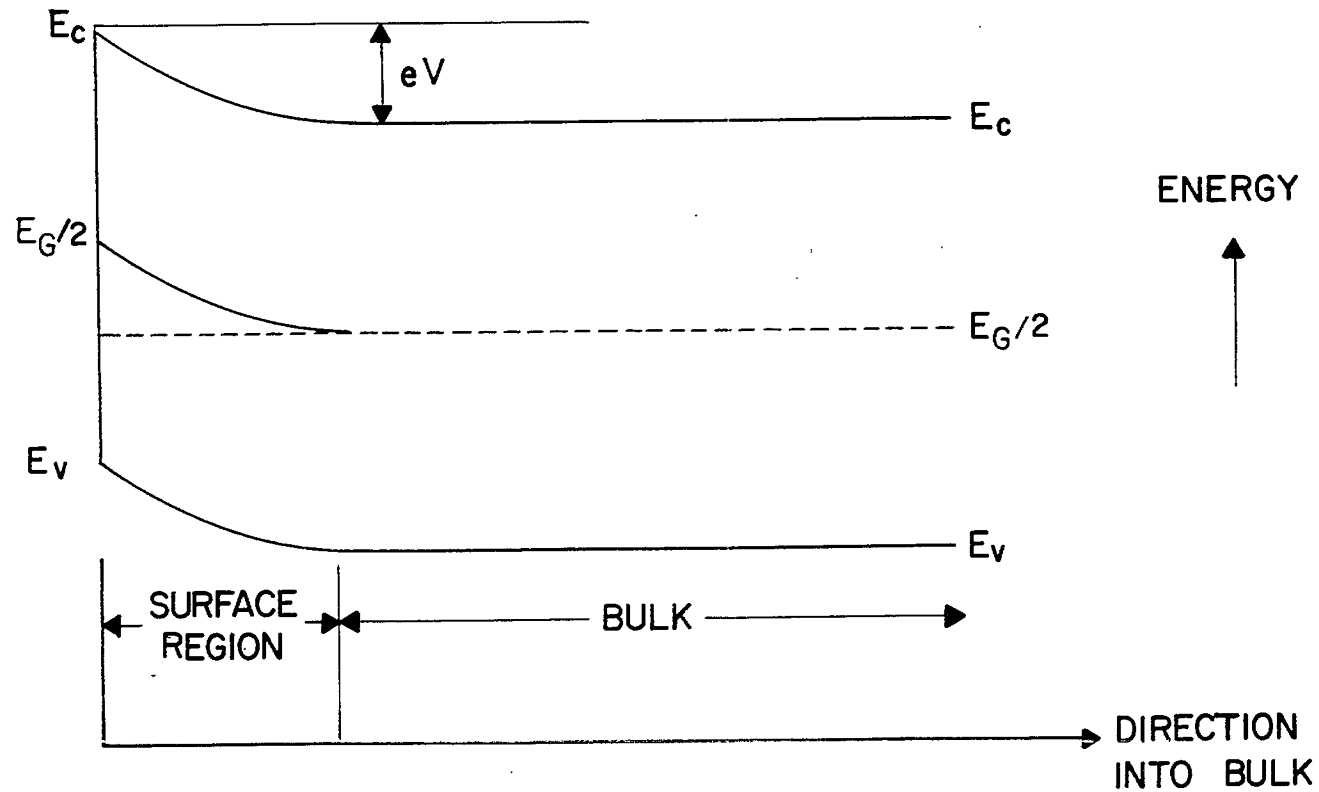

FIGURE 4. Energy-band diagram showing the potential change between the surface and bulk of an intrinsic semiconductor. Note that surface region exhibits p-type behaviour.

In theory, bulk-transport measurements will generally provide data on such semiconductor characteristics as volume resistivity, charge-carrier concentration, the effect of impurities, the thermal activation energy required for transport, the degree of scattering of charge carriers, the type of bonding, the thermoelectric power, and the effective masses of the charge carriers. Surface-transport measurements will give additional information, such as the space-charge capacitance, the potential between the bulk and surface, an indication of surface states, and the contact potential of the semiconductor across an interface formed with a metal or an electrolyte.

In practice, however, the detailed application of the transport theory of semiconductors to naturally occurring minerals has to be treated with caution, because of the variable and randomly distributed amounts of electrically active impurities that are usually present in minerals. However, in general, electrical transport studies do provide data that are qualitatively useful in describing the n- or p-character of a mineral, and in comparing samples of the same mineral from different locations within the same ore body, or of the same mineral from different geographical locations.

THE MEASUREMENT OF SEMICONDUCTOR PROPERTIES

The Problem of Ohmic Contacts

A major problem that exists with most types of electrical measurement on semiconductors is the making of a good ohmic contact to the specimen. An ohmic contact is defined as a contact that allows an unrestricted flow of majority charge-carriers (electrons or holes) across the interface and is such that the minority charge-carrier flow (holes or electrons) is negligible. This means that the applied potential will appear across the bulk of the material, rather than at the contact as in the case of

a rectifying junction. As a general rule, ohmic contacts require that the work function of the metal used to make the contact must be less than the work function of n-type semiconductors, and should be greater than the work function of p-type semiconductors (15). Energy-band diagrams are shown in Figures 5 and 6 for ohmic contacts to n- and p-type semiconductors respectively.

In the following description of various electrical measurements, it is assumed that ohmic contacts do exist.

Bulk-Property Measurements

1. Conductivity

Conductivity is defined as the proportionality constant between current density and the electric field, that is:

$$J = \sigma E \qquad \ldots \qquad \text{(Eq. 7)}$$

where J = current density in amp cm^{-2},
σ = conductivity in $ohms^{-1} cm^{-1}$, and
E = electrical field in volts cm^{-1}.

The current density for a hole charge-carrier system is given by:

$$J = pev_a \qquad \ldots \qquad \text{(Eq. 8)}$$

where p = number of hole carriers cm^{-3},
e = electronic charge (1.6×10^{-19} coulombs), and
v_a = average velocity of carriers in cm sec^{-1}.

Combining Equations 7 and 8 yields:

$$\sigma = pe \frac{v_a}{E}$$

which is generally given as

$$\sigma = pe\mu_p \qquad \ldots \qquad \text{(Eq. 9)}$$

where μ_p is defined as the carrier mobility of holes in $cm^2 volt^{-1} \text{-} sec^{-1}$. A comparable equation applies for electrons. Thus, if the mobility and conductivity are known, the number of charge carriers may be calculated.

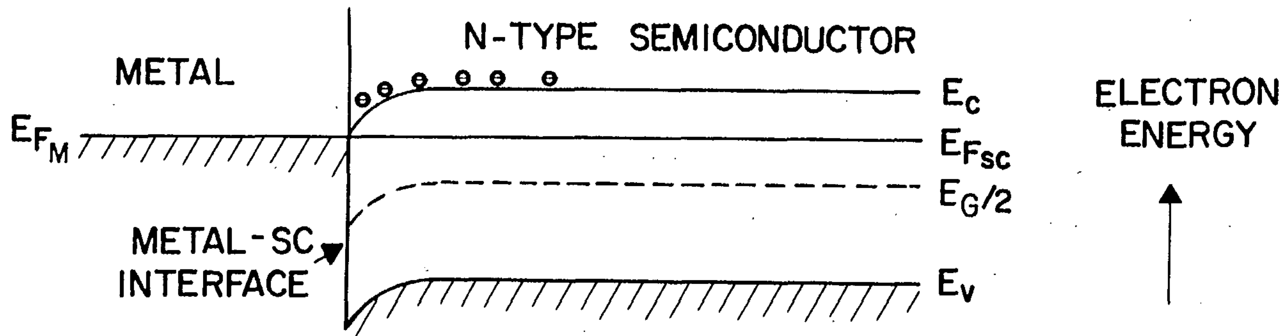

Note that there is no barrier hill to restrict the flow of conduction band electrons.

(a)

FIGURE 5. Energy-band diagram for an ohmic contact to an n-type semiconductor.

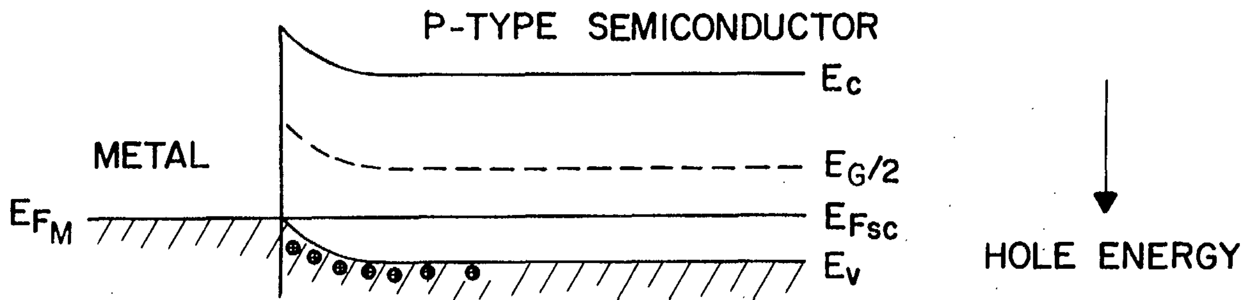

Note that there is no potential hill to restrict the flow of the valence band holes.

(b)

FIGURE 6. Energy-band diagram for an ohmic contact to a p-type semiconductor.

In the more general case, where both electrons and holes are involved in the conduction process, the conductivity is given by

$$\sigma = e(\mu_n n + \mu_p p), \qquad \ldots \qquad \text{(Eq. 10)}$$

where the subscripts "n" and "p" refer to electrons and holes, and n and p are the respective electron- and hole-concentrations.

Conductivity -- or its reciprocal, resistivity -- is a material constant (as compared to electrical resistance, which is a function of geometry) and can vary over about 25 orders of magnitude for different materials (5). It is usually measured in terms of resistance and sample geometry. Generally, a convenient sample size is approximately 1 cm x 0.25 cm x 0.1 cm. Careful cutting, shaping and parallel grinding, and accurate dimension measurements, are required. Single-crystal material is not necessary, in most circumstances. Measurement techniques (16-19) should be capable of ranging from 10^{-4} ohms (metals) to 10^{13} ohms (insulators); most semiconductor resistances are between these limits. It should be noted that the conductivity of semiconductors usually increases with increasing temperature.

2. Carrier Mobility

The mobility of charge carriers is obtained by Hall-effect measurements (6). Figure 7 shows the application of a magnetic field placed perpendicular to the current flow in a p-type sample. The magnetic flux deflects the current carriers and a restoring force (Hall potential) is created to maintain equilibrium. This is given as:

$$Bev = eE \qquad \ldots \qquad \text{(Eq. 11)}$$

where B = the magnetic-flux density in gauss,

e = the electronic charge in coulombs,

v = the velocity of the carriers in cm sec^{-1}, and

E = the Hall field in volts cm^{-1}.

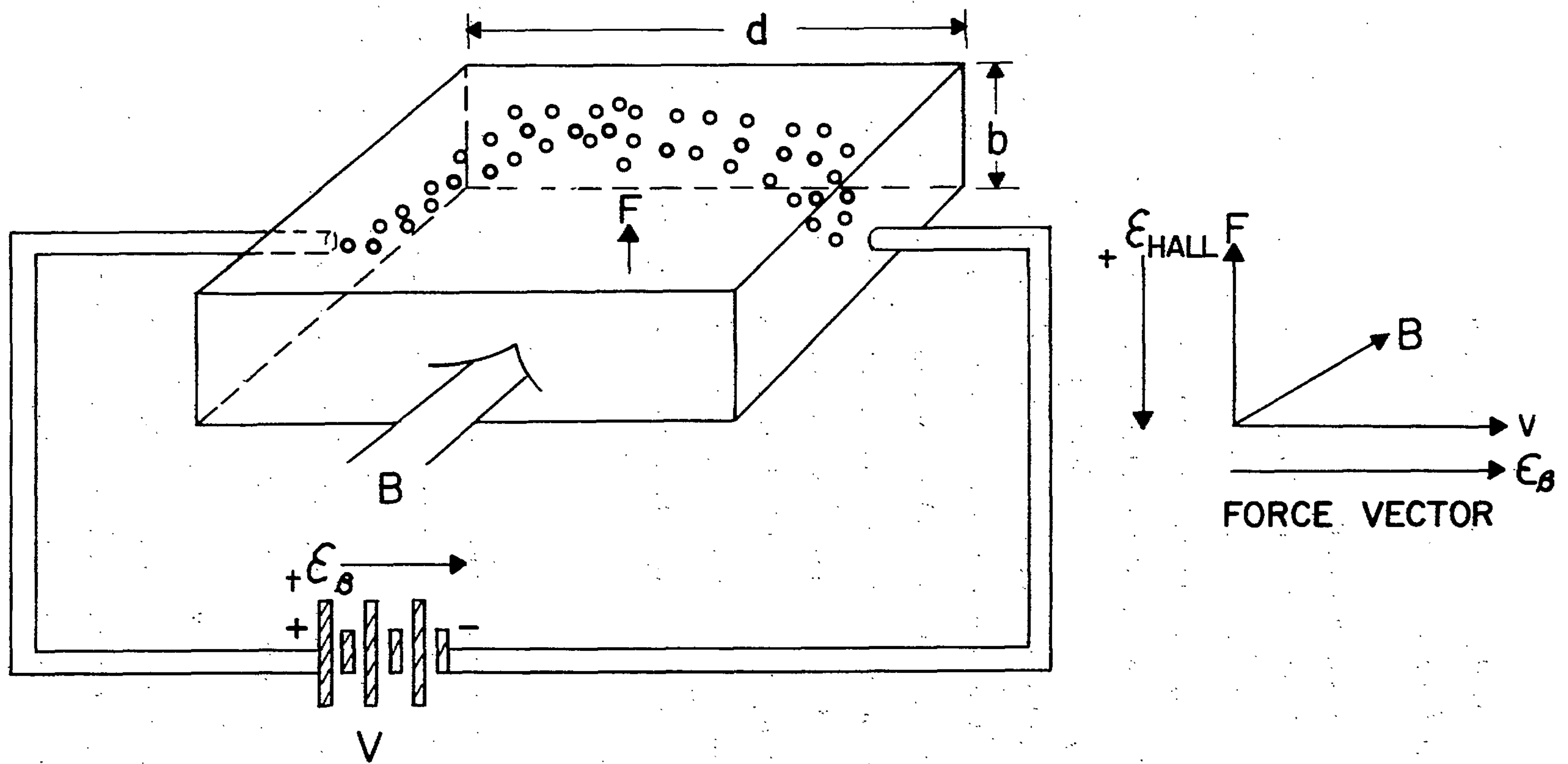

FIGURE 7. A diagrammatic view of the effect of a magnetic field on positive charge carriers in a crystal.

As the current carriers in Figure 6 are holes, the force equation is positive. In terms of sample geometry, the Hall voltage is:

$$V_H = \frac{BbJ}{pe} = R_H BbJ \qquad \ldots \qquad \text{(Eq. 12)}$$

where V_H = the Hall voltage,

R_H = the charge density in cm^3C^{-1},

J = the current density im amps cm^{-2}, and

p = the carrier concentration in carriers cm^{-3}.

Note that the Hall voltage is positive for hole carriers. If Equations 7 and 8 are combined, this gives the Hall mobility:

$$\mu = R_H \sigma \qquad \ldots \qquad \text{(Eq. 13)}$$

As the magnetic field deflects both electrons and holes in the same direction, the Hall potential only provides information on the resultant charge density in the sample being measured. Ideally, to measure mobility it is desirable to use materials that have only one type of charge carrier. First, intrinsic material is obtained. Then it is doped with either donor or acceptor atoms, making the material an n-type of a p-type semiconductor as required. (Stoichiometric deviations can also result in doping some cases, e.g. PbS (20).) Mobility measurements for electrons or holes may then be made on the doped material with negligible interference from minority carriers.

For mobility measurements using an intrinsic or a compensated semiconductor (a material which contains both donors and acceptors) where both holes and electrons must be taken into account, the resultant charge density is (6):

$$R_H = -\left(\frac{3\pi}{8e}\right)\frac{nc^2 - p}{(nc + p)^2} \qquad \ldots \qquad \text{(Eq. 14)}$$

where $c = \mu_n/\mu_p$. Before the mobility of each type of charge carrier can be obtained, a further relationship has to be found between n and p. This is usually done by varying the impurity concentrations and measuring the mobility at very low temperatures and then extrapolating the results to higher temperatures where intrinsic behaviour predominates.

Mobility is a characteristic of the conduction and valence bands of the material and indicates the degree of scattering encountered by the current-carrying electrons or holes. It is temperature-dependent, usually obeying a T^{-n} relationship, where n is less than three (6, 21). In a limited sense, mobility can also determine the nature of the bonding in a semiconductor, as a function of temperature (22).

The sample size required for mobility measurements is similar to that required for conductivity measurements. Instruments used to measure mobilities have a sensitivity limit of about $10^{-5} cm^2 volt^{-1}-sec^{-1}$ for high-conductivity material and $10^{-7} cm^2 volt^{-1}-sec^{-1}$ for low-conductivity material. A good account of various Hall-effect measuring techniques is given by Putley (6).

3. Fermi Energy and Activation Energy

For intrinsic semiconductors, or for doped semiconductors operating in their intrinsic regions, the Fermi level is approximately half-way between the bottom of the conduction band and the top of the valence band (5, 22). The exact energy level is given by:

$$E_F = (E_C - E_V)/2 + 3/4\ kT \ln m_n^*/m_p^* \qquad \ldots \quad \text{(Eq. 15)}$$

For a doped semiconductor (e.g. extrinsic n-type) at low temperature, the Fermi level lies half-way between the average concentration of donor-atom states and the bottom of the conduction band. As the temperature of the semiconductor is increased, the Fermi level lowers as the atoms in the donor levels become depleted of electrons, and conduction electrons start to come from the valence band (Figure 8). Figure 9 shows the relationship between the extrinsic and the intrinsic carrier concentrations as a function of temperature.

The energy required to excite an electron into the conduction band or create a hole in the valence band is called the activation energy.

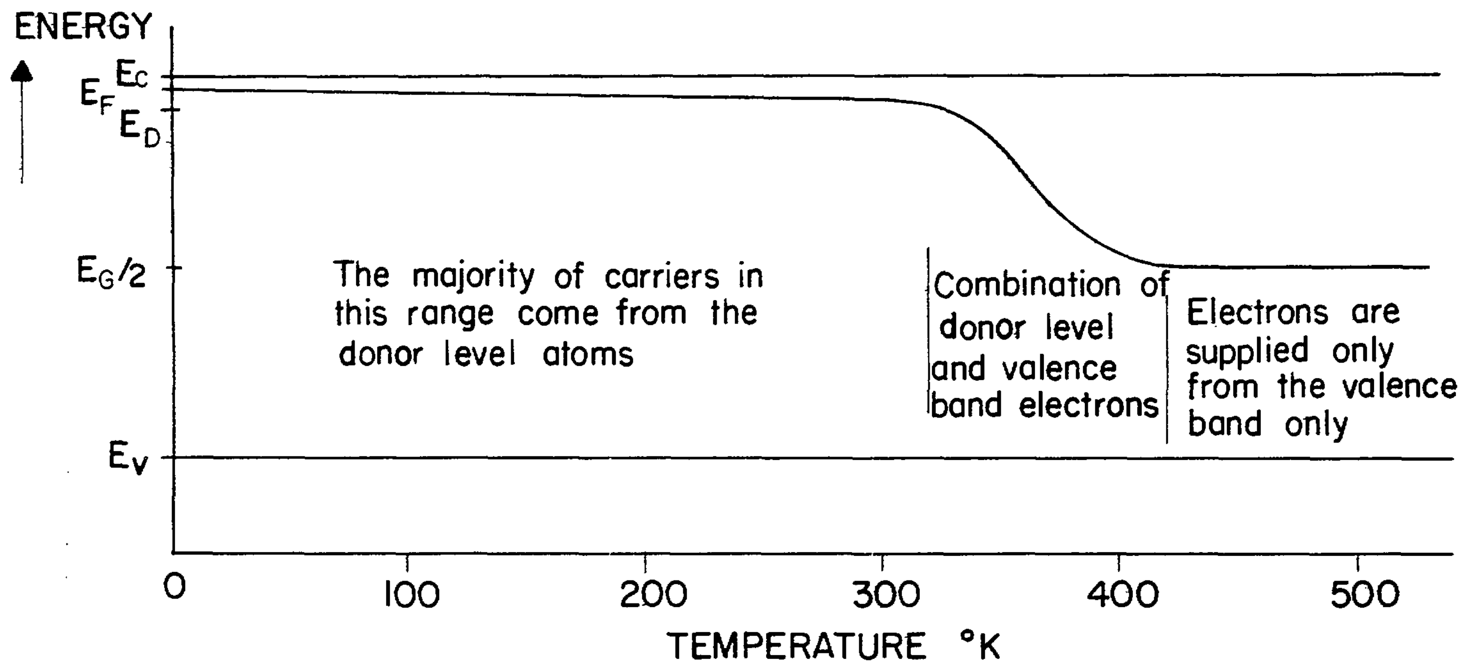

FIGURE 8. Fermi-energy level versus temperature for a typical n-type semiconductor.

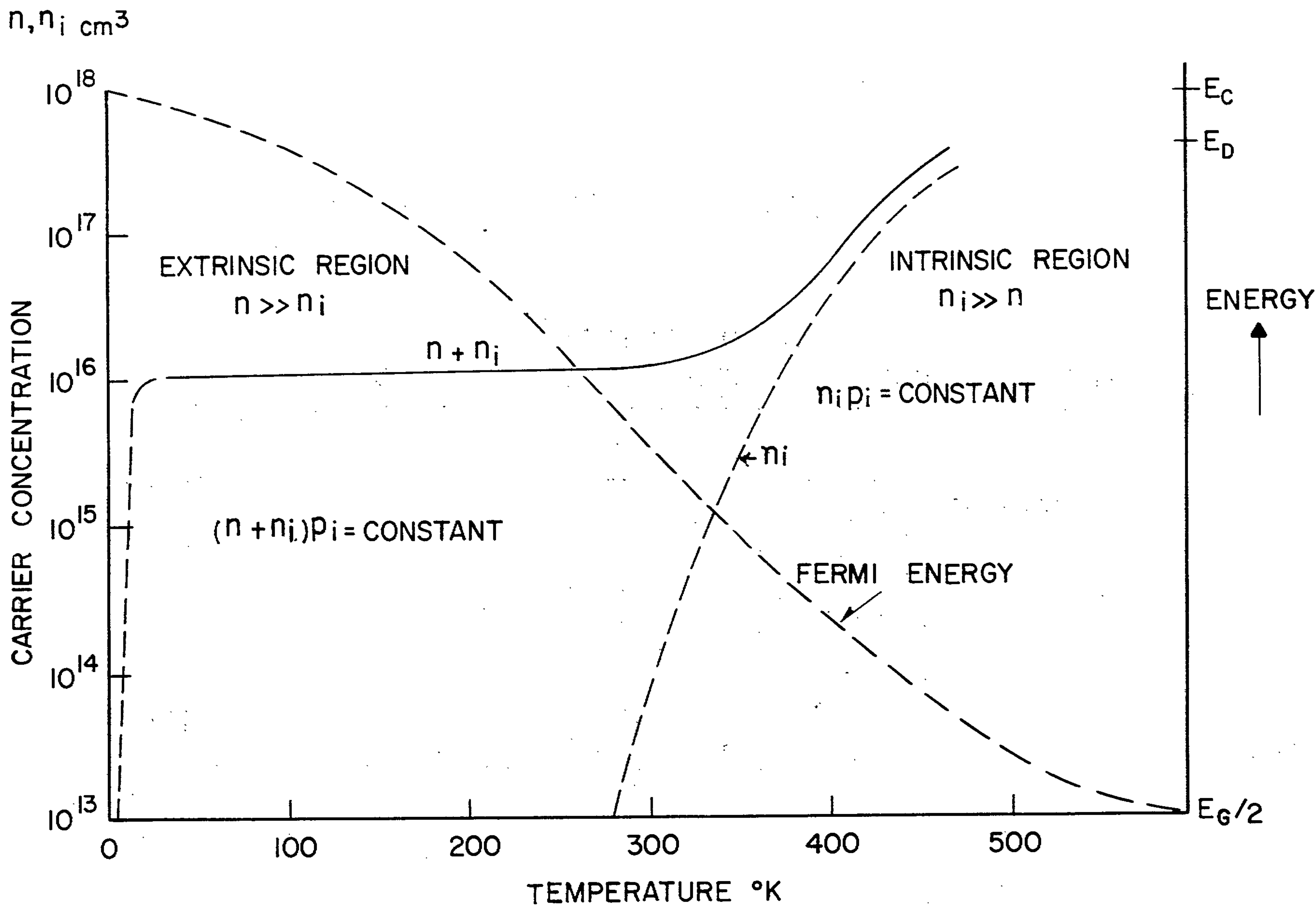

FIGURE 9. Intrinsic and extrinsic carrier concentration versus temperature of a typical n-type semiconductor.

When the carrier concentration from Equation 5 is substituted in Equation 9, it will be seen that the conductivity is an exponential function of $E_F - E_V$. If $\ln \sigma$ is plotted versus $1/T$, the resulting slope yields the activation energy (over a small temperature range) which is obtained from the following relationship:

$$\frac{(E_F - E_V)}{kT} = \frac{2.3 \, \Delta \log \sigma}{\Delta \frac{1}{T}} \quad \ldots \quad \text{(Eq. 16)}$$

As intrinsic conductivity is approached, the activation energy $(E_F - E_V)$ approaches $E_G/2$. A similar relationship exists for n-type material.

4. Thermoelectric Power

The thermoelectric power of a material is a measure of the tendency of mobile charge carriers to move from the hot end to the cold end of a sample, when the sample is placed in a temperature gradient. The charge-carrier flow results in the establishment of a restoring force (Seebeck voltage) to maintain the net current as zero. The thermoelectric power Φ_T, is given in volts $°K^{-1}$ as the temperature gradient across the sample tends to zero. Therefore, it is necessary to measure thermoelectric voltages with the smallest possible temperature gradient (6, 23-26).

Electrons give rise to negative thermoelectric voltages; thus, the thermoelectric power has a negative sign, and is given by (24):

$$\Phi_T = -\frac{k}{e} \left\{ A - \frac{(E_C - E_F)}{kT} \right\} \quad \ldots \quad \text{(Eq. 17)}$$

where Φ_T = thermoelectric power in volts $°K^{-1}$ at a temperature T in °K, and

A = a constant (usually ~ 2).

An important aspect of the thermoelectric power relationship (Equation 17) is that it contains the activation energy that is necessary to determine charge-carrier concentrations given in Equations 4 and 5. Combining Equation 17 with Equations 4 and 5 gives the value of the effective density-of-states mass of the charge carrier (Equations 2 and 3). The effective density-of-states mass enables the carrier concentration to be calculated with better accuracy.

The density-of-states mass can also be used to determine the degree of anisotropy of the energy surfaces (k space) of the solid; however, the models used for this theory (4, 6) are quite complex and beyond the scope of this report.

Energy-Barrier Measurements

1. Semiconductor-Metal Contact

When a metal and a semiconductor are isolated from each other, the only common energy-boundary condition that exists between them is the zero-energy reference value of their work functions (7). When the metal is isothermally in contact with the semiconductor, the Fermi energy level of the metal and the Fermi energy level of the semiconductor must finally come to the same energy value. In order to maintain these two energy conditions when a metal-semiconductor contact is made, a redistribution of charge has to take place at the interface. Because the semiconductor can only supply (or contain) a small number of charge carriers per unit volume, compared with the metal, the semiconductor has to deplete (or store) charge carriers for a significant distance from its surface (~1 micron). The semiconductor can accommodate a decrease or increase in the number of charge carriers only by the bending of its conduction and valence energy-bands. The redistribution of charge in the surface region of the semiconductor appears as a macroscopic potential across the so-called space-charge region from which the entire surface-barrier potential is measured (27-29). The surface-barrier potential is given, by definition (7), as:

$$-eV_D = \theta_M - \theta_{SC} \text{ (n-type material)} \qquad \ldots \qquad \text{(Eq. 18)}$$

where $-V_D$ = the surface-barrier potential,

θ_M = the work function of the metal, and

θ_{SC} = the work function of the semiconductor.

Equation 18 can be rearranged to:

$$-eV_D = \theta_M - \chi_{SC} - (E_C - E_F) \qquad \ldots \qquad \text{(Eq. 19)}$$

where

$$\theta_{SC} = \chi_{SC} + (E_C - E_F) \qquad \ldots \qquad \text{(Eq. 20)}$$

and where χ_{SC} is the electron affinity of the semiconductor, i.e., the energy required to remove an electron from the conduction band and place it at a point in free space just outside the semiconductor (7). In most cases, the junction formed by a metal in contact with a semiconductor behaves electrically as a voltage-dependent capacitance. A capacitance exists (4, 7, 28, 29) because of the space-charge potential that is developed to maintain charge equilibrium (Figure 10). For such a system it may be shown that (29):

$$\frac{1}{C^2} = \frac{2(V_D - V)}{e\epsilon\epsilon_0 n A^2} \qquad \ldots \qquad \text{(Eq. 21)}$$

where A = contact area in cm^2,

C = barrier double-layer capacitance in farads cm^{-2},

V_D = surface-barrier voltage in volts,

V = applied bias voltage,

ϵ = dielectric constant of the semiconductor,

ϵ_0 = permittivity of free space (8.85×10^{-14} farad cm^{-1}), and

n = bulk density of donors (or p for acceptors) in carriers cm^{-3}.

Thus, the density of donors and the surface-barrier voltage may be determined from the slope and the intercept of a graph of $1/C^2$ versus the bias voltage, V (Figure 11). Goodman (30, 31) gives a good account of this type of measurement.

Energy-band diagrams are shown in Figures 12, 13, 14 and 15 for n-type and p-type semiconductors in contact with metals whose work functions are greater than or less than the work function of the semiconductors. Note that when the position of the Fermi level in the surface region of the semiconductor approaches $E_G/2$ for both n-type and p-type semiconductors, a region depleted of charge carriers exists, and hence a surface barrier is formed. When the position of the Fermi level in the surface region moves towards the conduction-band edge for n-type semiconductors, or towards

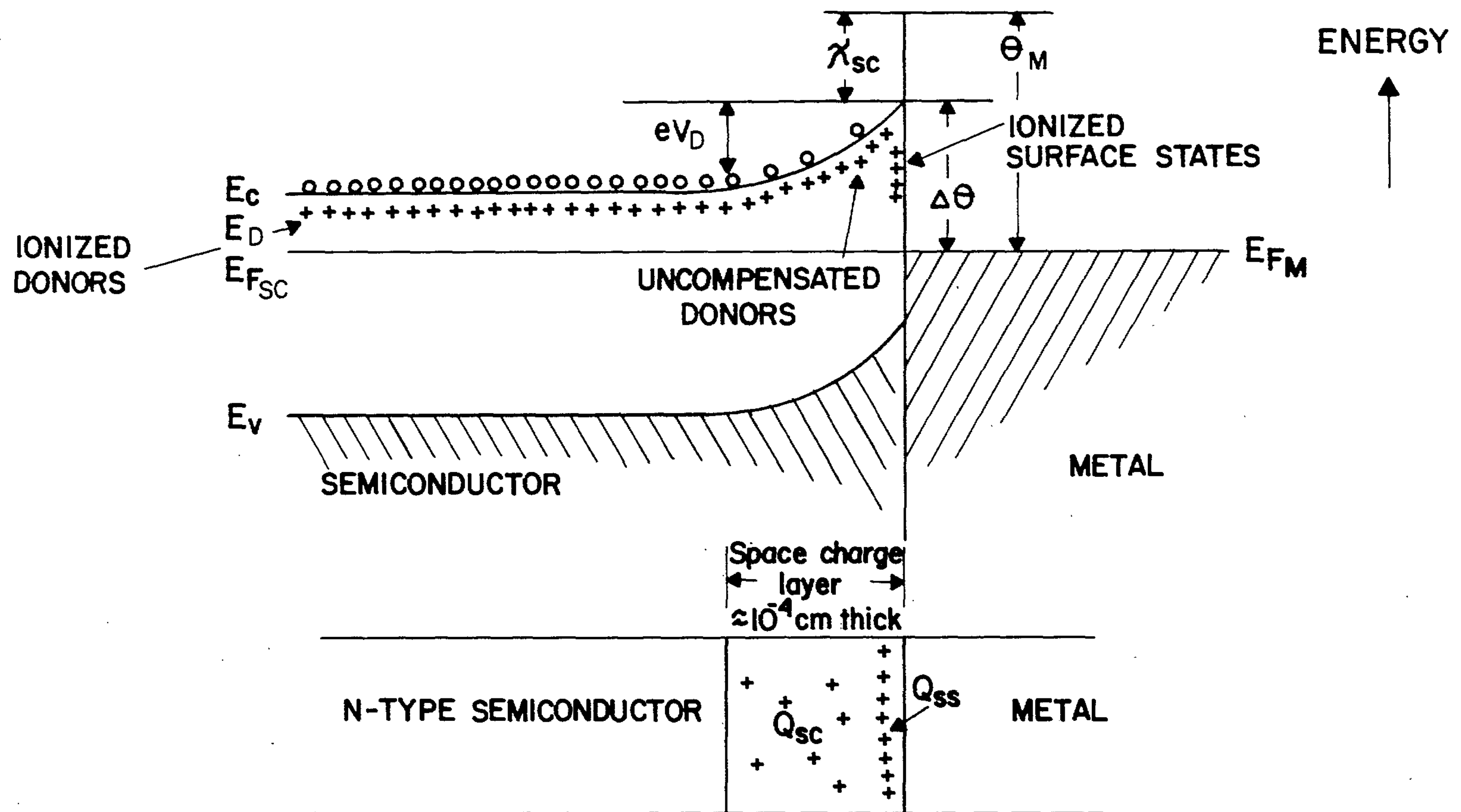

FIGURE 10. Schematic structure and energy-level diagram of a typical n-type semiconductor/metal interface.

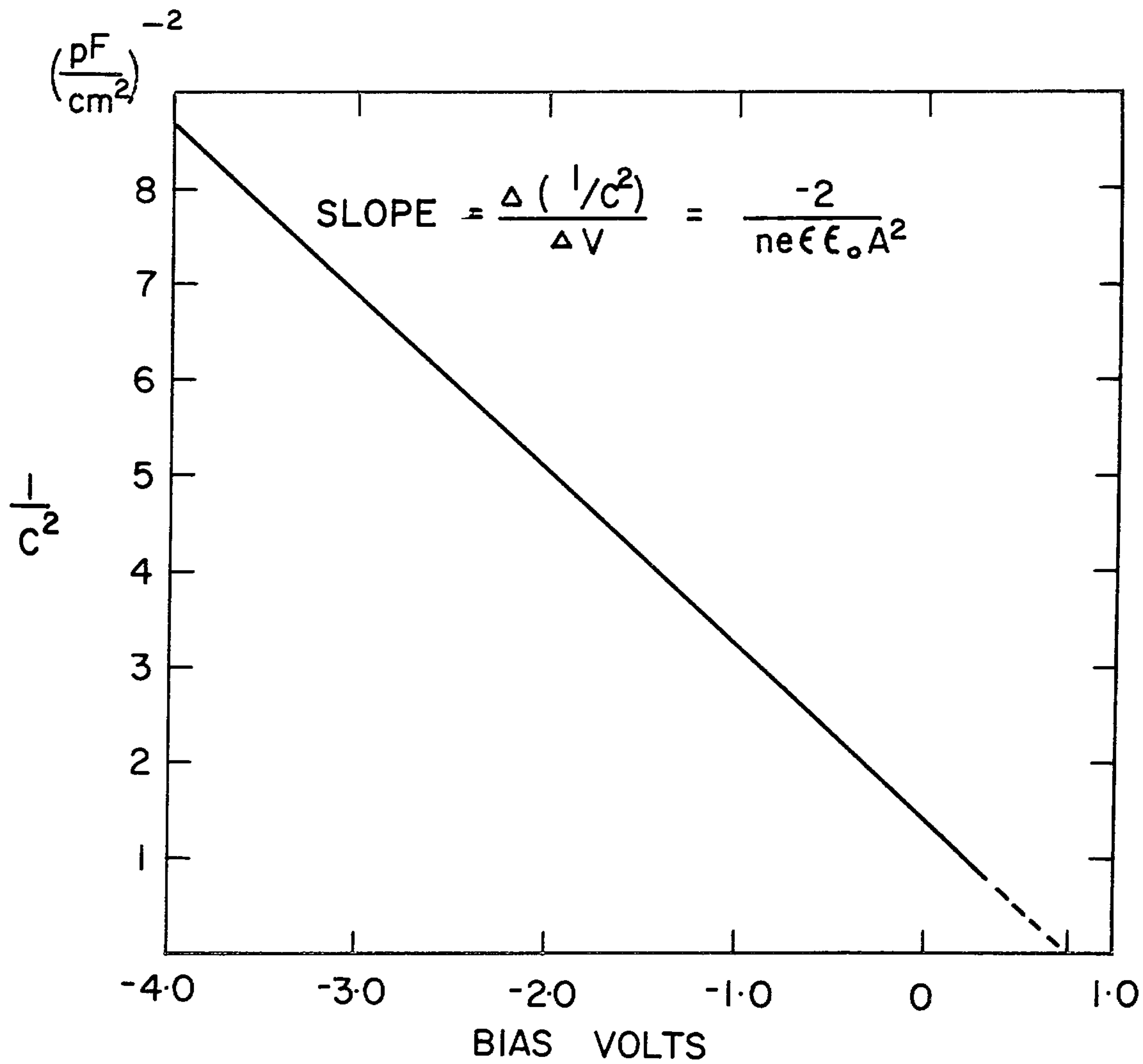

FIGURE 11. Variation of $1/C^2$ versus bias voltage CdS/Au interface (after Goodman, A. ref. 30-31).

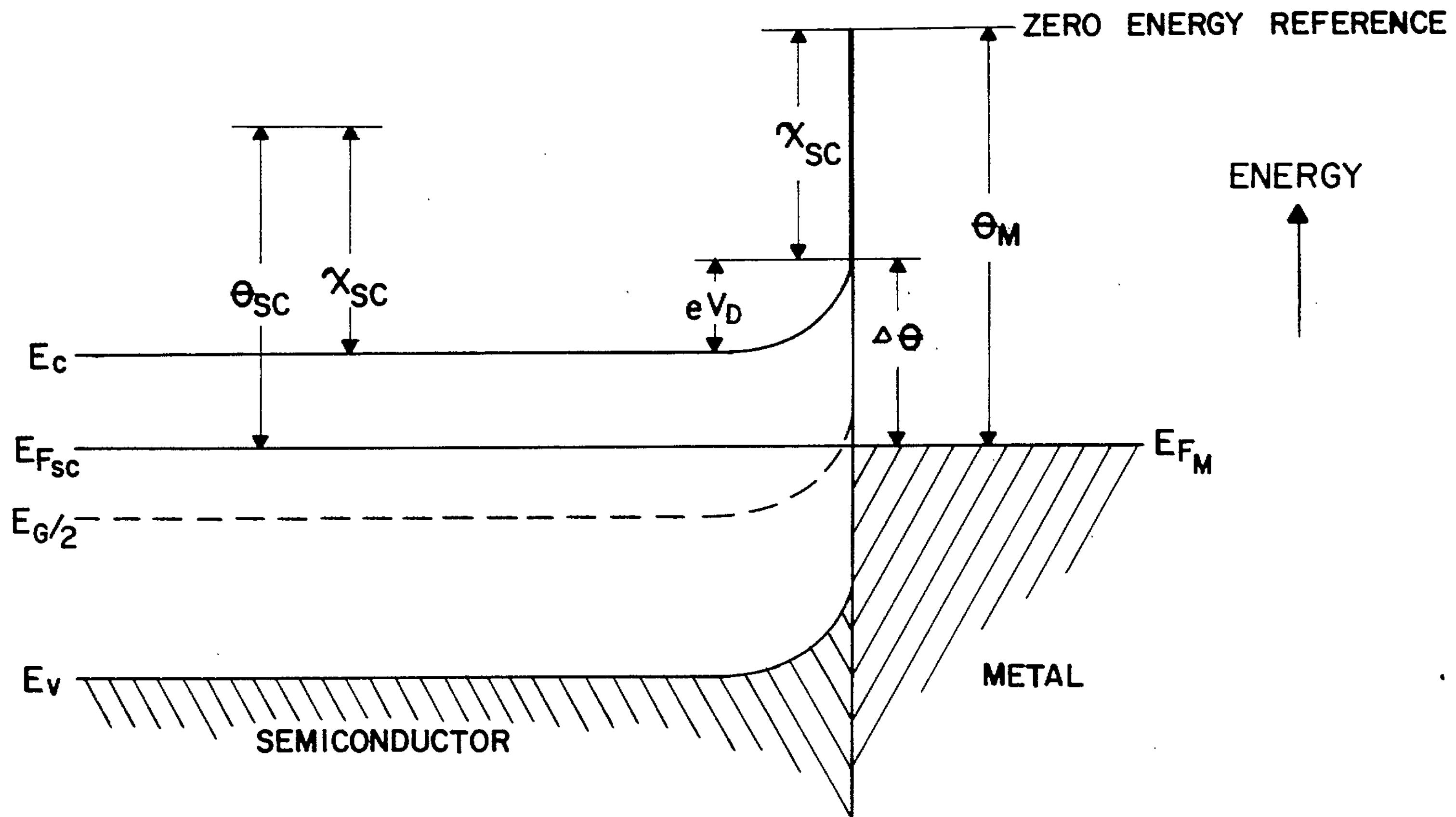

FIGURE 12. Energy-band diagram for an n-type semiconductor/metal interface where $\Theta_M > \Theta_{SC}$. A potential barrier $-eV_D$ exists, giving a rectifying contact.

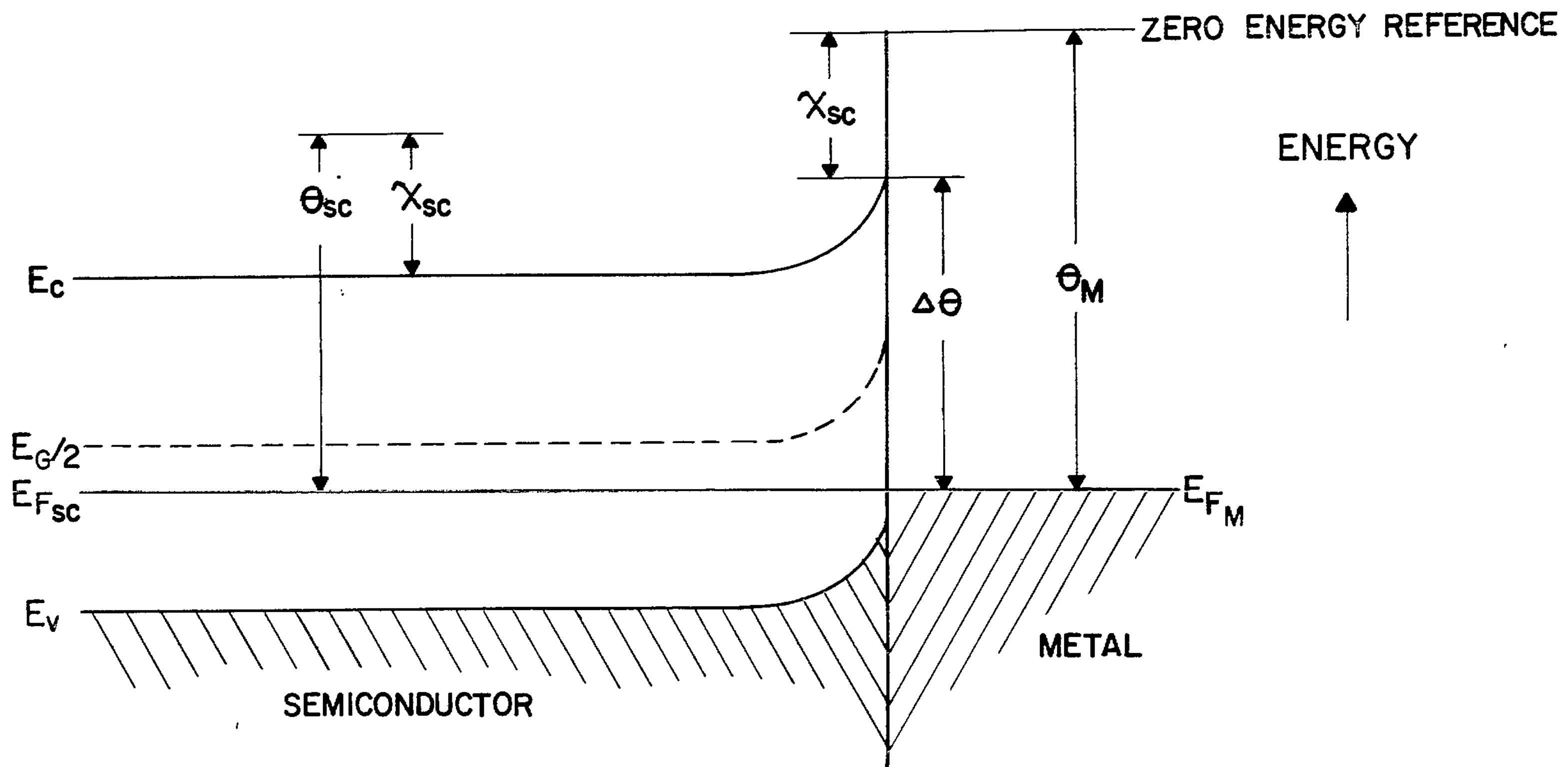

FIGURE 13. Energy-band diagram for a p-type semiconductor/metal interface where $\theta_M > \theta_{SC}$. An accumulation region of positively charged carriers exists at the interface, resulting in an ohmic contact.

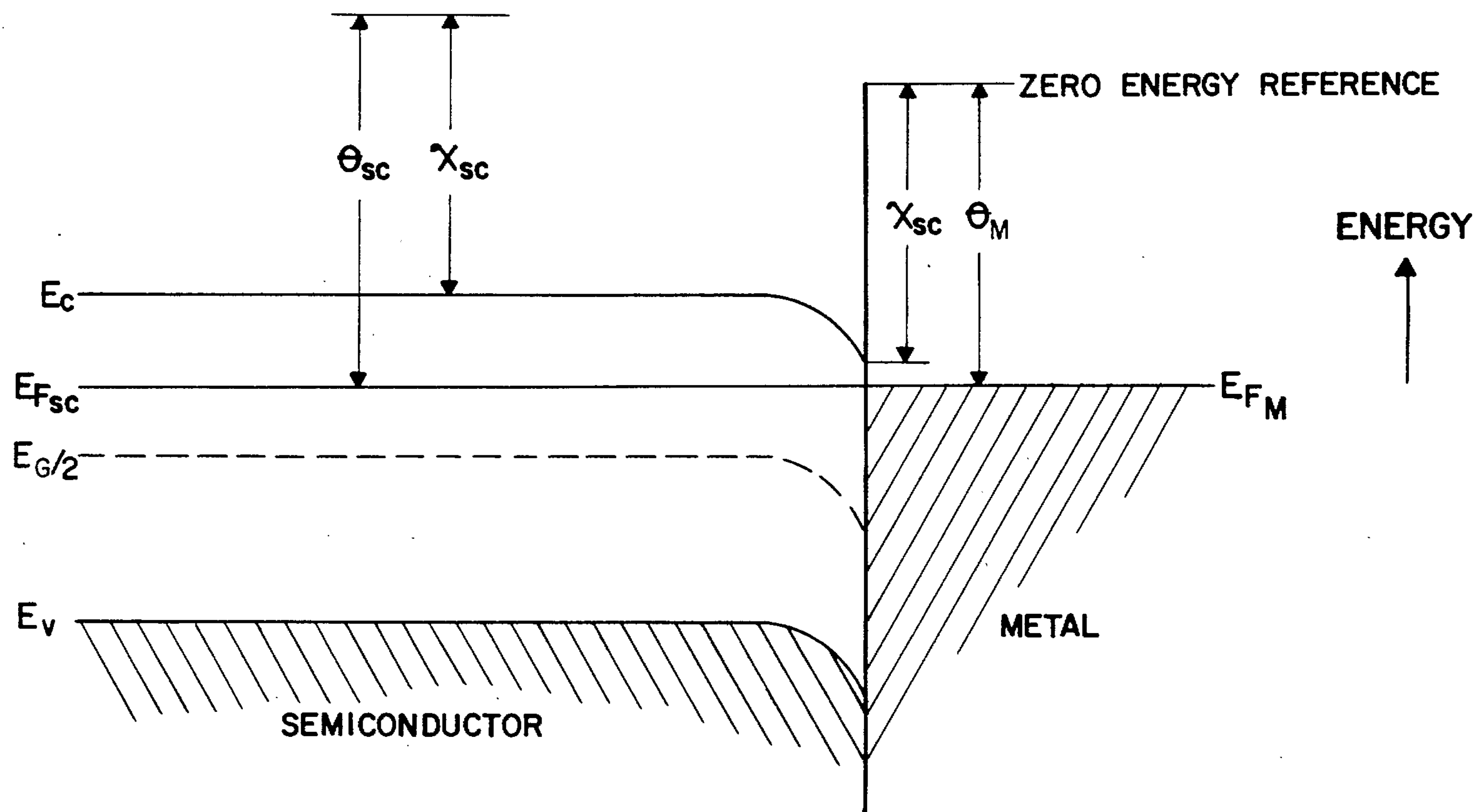

FIGURE 14. Energy-band diagram for an n-type semiconductor where $\theta_{SC} > \theta_M$. An accumulation region of negatively charged carriers exists at the interface resulting in an ohmic contact.

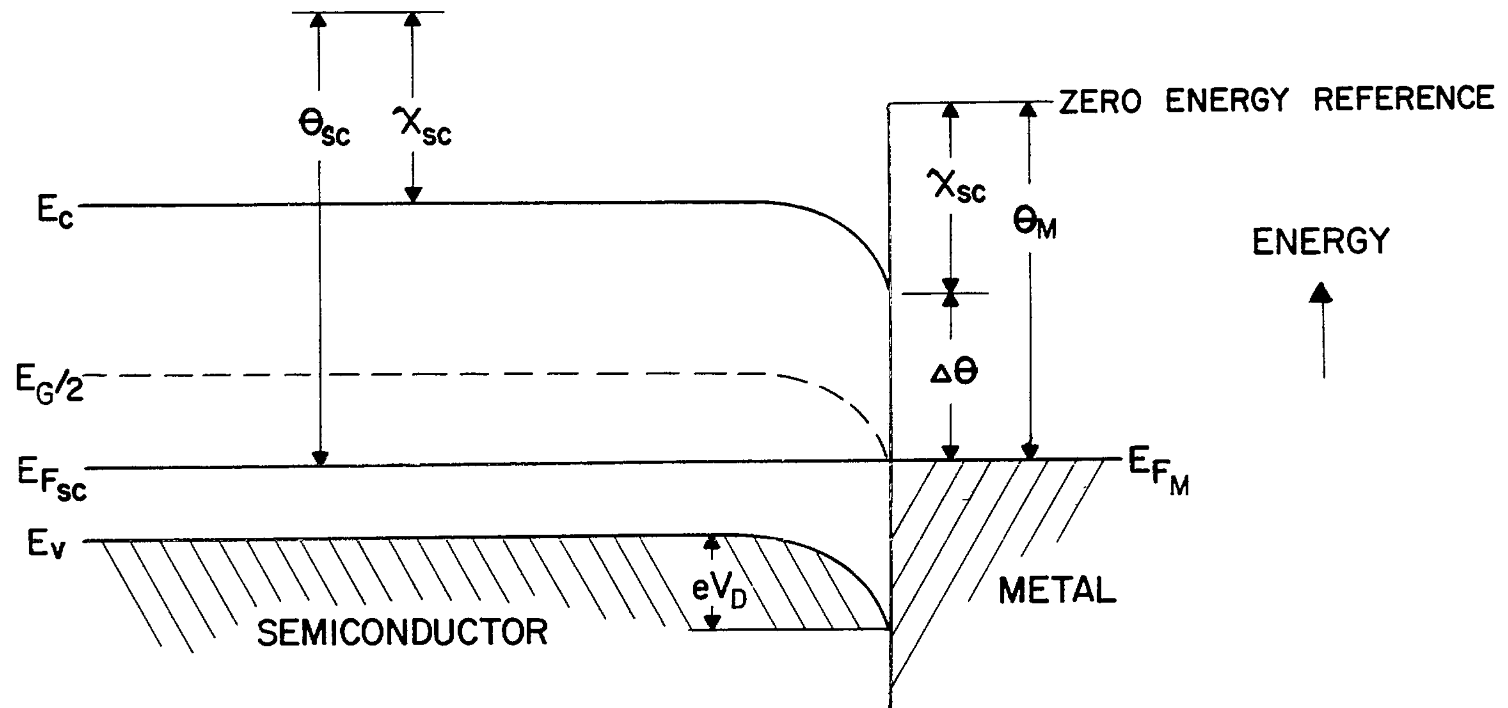

FIGURE 15. Energy-band diagram for a p-type semiconductor/metal interface where $\Theta_{SC} > \Theta_M$. A potential barrier eV_D exists, giving a rectifying contact.

the valence-band edge for p-type semiconductors (compared with the Fermi level position in the bulk), this denotes a charge-carrier accumulation and ohmic contacts can result.

From Figures 12 and 14, the magnitude of the barrier height, $\Delta\theta$ (which is the difference between the work functions of the metal and the semiconductor), is given as:

$$\Delta\theta = \theta_M - \theta_{SC} \qquad \ldots \qquad \text{(Eq. 22)}$$

The barrier height can be obtained from the saturation current density, J_o, as described in simple diode theory (15). The current density in a junction is given as:

$$J = J_o \left[\exp \frac{+eV}{kT} - 1 \right] \qquad \ldots \qquad \text{(Eq. 23)}$$

where J = the current density in amps cm^{-2}, and

V = the applied bias voltage.

The barrier height potential, $\Delta\theta$, can be obtained from the saturation current density which is given by

$$J_o = \left[\frac{4\pi m^* e k^2 T^2}{h^3} \right] \exp \frac{-e\Delta\theta}{kT} \qquad \ldots \qquad \text{(Eq. 24)}$$

A plot of ln J versus bias voltage will give the experimental value of the barrier-height potential. This is done by extrapolating the linear portion of the ln J value to the abscissa where $V = \theta$. At this point, $J = J_o$. A volt-ampere characteristic of a p-type PbS/Al interface is shown in Figure 16. Figure 17 shows the plot of ln J versus V and the extrapolated value of ln J_o. The result is a barrier-height potential of 0.115 eV.

The barrier height can also be obtained from the following relationships (see Figures 12 and 15):

$$\Delta\theta = (E_C - E_F) + |eV_D| \quad \text{n-type material} \qquad \ldots \qquad \text{(Eq. 25)}$$

and

$$\Delta\theta = (E_C - E_F) - |eV_D| \quad \text{p-type material} \qquad \ldots \qquad \text{(Eq. 26)}$$

Surface-barrier measurements are usually made with a resistance-capacitance bridge to obtain the space-charge potential and the space-charge capacitance (30). The barrier-height potential is obtained from a volt-ampère plot, using reasonably sensitive voltmeters (~1 millivolt) and ammeters (~ 10^{-6} amperes).

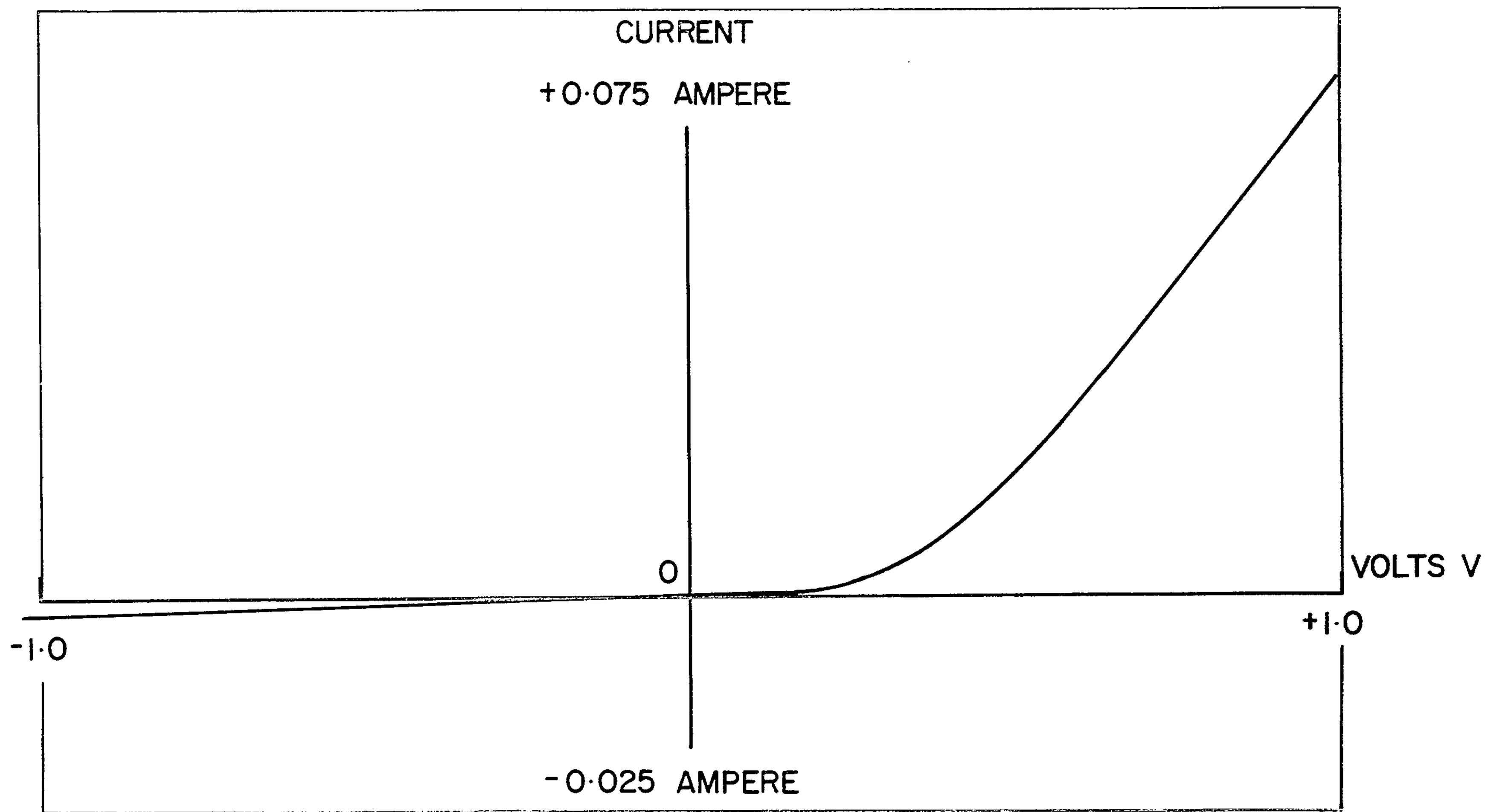

FIGURE 16. Voltage-current characteristic of a p-type PbS/Al contact at 77° K.

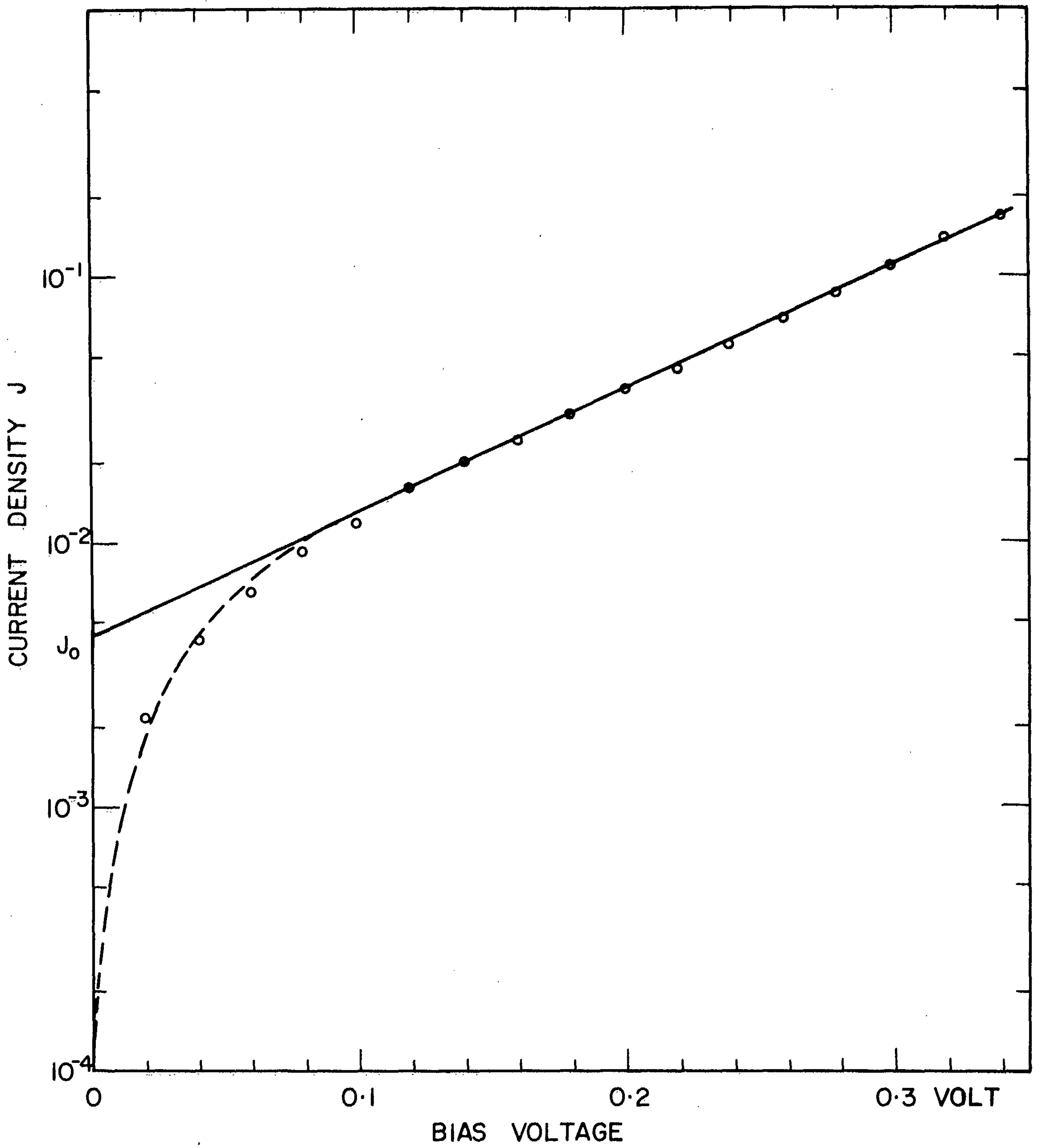

FIGURE 17. Log J versus bias voltage of a PbS/Al interface. PbS is p-type.

2. Semiconductor-Electrolyte Interface

When a semiconductor is placed in contact with an electrolyte, charge rearrangement occurs between the two phases until an equilibrium potential (the Galvani or inner potential) is established (32) between the bulk of the semiconductor and the interior of the solution (Figure 18). This charge rearrangement is associated with capacitances at the liquid side and the solid side of the interface. The liquid side, as is well known from electrochemical studies at the metal-solution interface (33), has two capacitances in series: the Helmholtz capacity (C_H) arising from a monolayer of adsorbed water dipoles and/or chemisorbed ions next to the solid phase, and the Gouy capacity (C_G) arising from the much more diffuse Gouy layer which can extend for a considerable distance into the solution. The total capacity of the liquid phase is given by:

$$\frac{1}{C_L} = \frac{1}{C_H} + \frac{1}{C_G} \qquad \text{... (Eq. 27)}$$

For solutions of reasonable concentration (greater than 0.1N), the capacity of the Gouy layer is much larger than that of the Helmholtz layer and the latter effectively gives the capacity of the solution side of the double layer. Most experimental measurements of capacity are performed under these conditions (32).

Neglecting for the moment the possible presence of surface states in the semiconductor, there will be a capacity in the semiconductor due to the space-charge region (C_{SC}). Thus the total capacity of the semiconductor-electrolyte interface is given by:

$$\frac{1}{C_T} = \frac{1}{C_{SC}} + \frac{1}{C_H} + \frac{1}{C_G} \qquad \text{... (Eq. 28)}$$

In general, the measured capacity (C_T) is governed by the value of the smallest capacity in Equation 28. For most cases this is the value of the space-charge capacitance, C_{SC}; a conclusion that may be reached from a consideration of the Debye lengths for the different charged regions (34). If surface states are present on the surface of the semiconductor, an

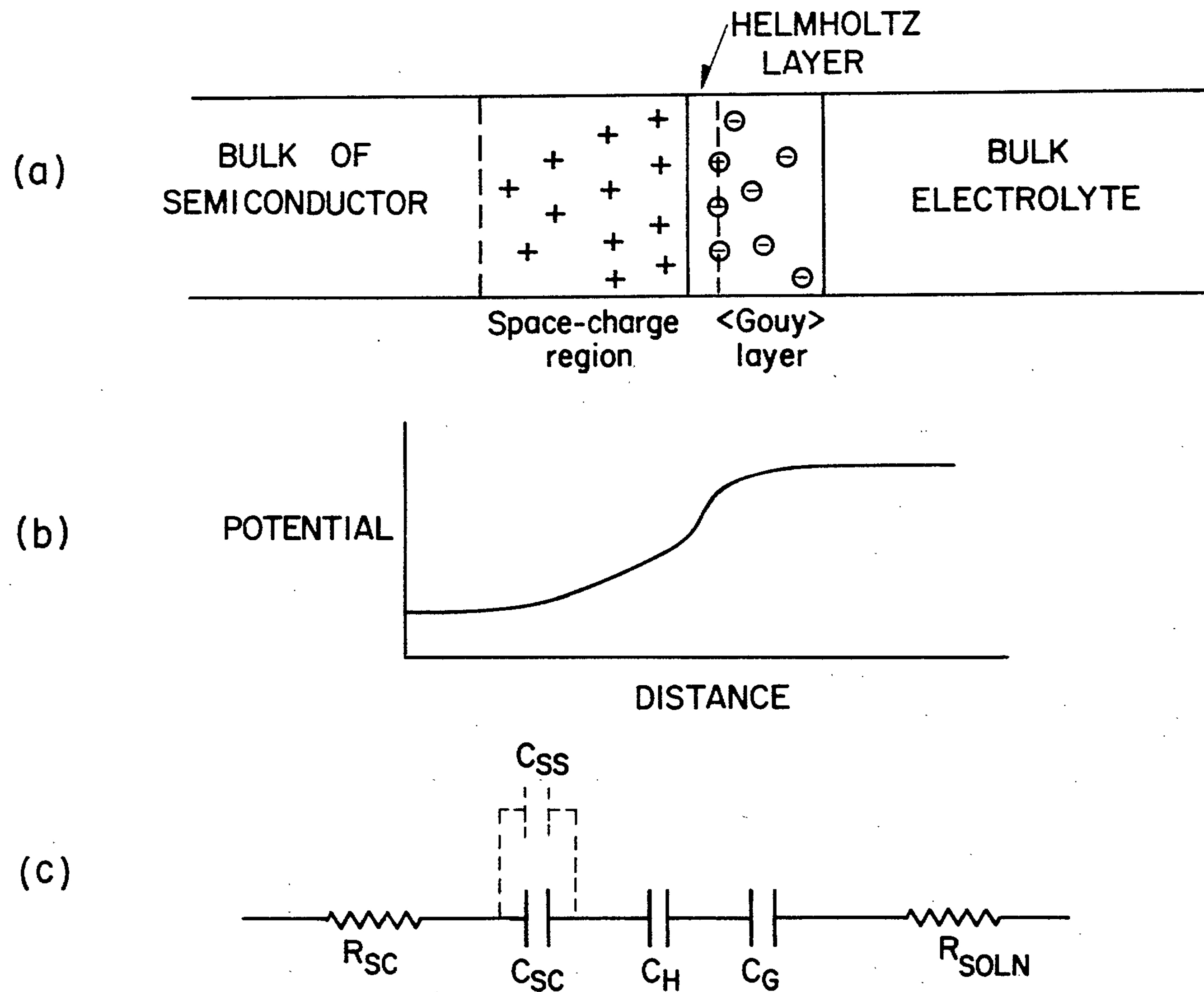

FIGURE 18. Structure of the double layer (a), potential distribution (b) and equivalent circuit (c), at the semiconductor-electrolyte interface.

additional capacity (C_{SS}) exists due to these surface states. This capacitance is in parallel with the space-charge capacitance (32) and Equation 28 is modified to give

$$\frac{1}{C_T} = \frac{1}{C_H} + \frac{1}{C_G} + \frac{1}{C_{SC} + C_{SS}} \quad \ldots \quad \text{(Eq. 29)}$$

A comparison of the measured capacitance with the calculated space-charge capacitance (7) allows the contribution of surface states to be estimated. For some systems, e.g. ZnO/electrolyte, no surface states were found (32). It should be noted that in some cases the interpretation of capacitance data is complicated by the flow of current across the interface, which results in electrochemical reactions and changing interfacial conditions. Since the attachment of flotation reagents is intimately associated with the charge distribution across the solid-liquid interface, capacitance measurements can provide an insight into the mechanism of attachment.

Surface Property Measurements

If a high voltage is placed parallel to a semiconductor surface, it will force the current carriers in the semiconductor to flow in the surface region. This behaviour is to be expected, as the forces involved are electrostatic and consequently attract or repulse charge. This effect, called the field-effect (7, 11), can be employed to characterize only the surface region of the semiconductor, using the same measuring techniques used for bulk-property characterization.

An important property of the surface region is the number and type of surface states that may exist. These states are charge-carrier traps and cause a space-charge potential to exist between the bulk and the surface region. Alternating-current fields and direct-current fields can be used to indicate fast states, that is, states closest to the bulk and which are a material property (known as Tamm states), or slow states, that is, states closest to the surface and which show the presence of defects and/or of adsorbed impurities (7, 11).

SOME APPLICATIONS OF SEMICONDUCTOR PRINCIPLES

As has been noted in earlier sections, the Fermi level is the electrochemical potential of electrons in a semiconductor; and from thermodynamic reasoning, when two different phases (or two different materials) are in contact and in thermal equilibrium, the Fermi levels of the two phases (or the two materials) will be equal when the free energy of the system is a minimum. Since the position of the Fermi level in the semiconductor is a function both of temperature and of impurity content, some control may be exercised over the thermodynamic and transport properties of electrons in the semiconductor.

An appreciation of the significance of the position of the Fermi level may be gained by considering the adsorption of an electronegative molecule, such as oxygen, on the surface of a semiconductor. If the work function of the semiconductor (Θ_{SC}) is less than the electron affinity (E. A.) of the oxygen molecule, it is energetically feasible for an electron to be transferred from the semiconductor to the oxygen molecule, and oxygen will be adsorbed on the semiconductor surface, with E. A. - Θ_{SC} giving a measure of the energy of adsorption. However, in the situation where E. A. $< \Theta_{SC}$, there is no tendency for electron transfer to occur and oxygen adsorption will not take place. From a chemical point of view, when the Fermi level in a given semiconductor is close to its conduction band (Figure 2), this n-type semiconductor may be regarded as a reducing agent (i. e. gives up electrons fairly readily) when compared to the same semiconductor with the Fermi level close to the valence band (Figure 3). By this analogy the latter case would correspond to an oxidizing agent, i. e., it would be more favourable for the p-type semiconductor to accept, rather than donate, electrons. This qualitative picture of electron transfer for gas-solid

interaction with semiconductors has been widely used in the description of catalytic behaviour (35). Similar reasoning may also be applied to the interaction of ions in solution with semiconductors, except that in this case the energy of hydration of the ions is an additional energy term to be considered. For a given semiconductor, assuming that other conditions remain constant, one would expect in general that chemisorption of an anion would be favoured by p-type conductivity, and chemisorption of a cation by n-type conductivity. An interesting aspect of semiconductor-ion interaction is the flotation process, where a chemisorption bond is required between the collector-ion and a semiconducting mineral. By suitable treatment it is possible to modify the surface region of the mineral relative to the bulk. Thus, it is possible to create an n-type surface on a p-type mineral, and vice versa. Since the interaction of the collector in solution is only with the surface region of the mineral, correct surface pretreatment will permit control in flotation by modifying the interfacial energetics of the solute-ion/solid-surface interaction. In the section on metal-semiconductor contacts (page 20) it was shown that, depending on the Fermi levels (work functions) of the metal and the semiconductor, the surface region of an n-type semiconductor can be changed to p-type by contact with a metal of lower work function (Figure 12), the metal in this case acting in the general sense as an oxidizing agent. This same effect may, of course, be obtained in other ways. For example, the treatment of an n-type material with an oxidizing agent, such as hydrogen peroxide, will tend to remove electrons from the semiconductor and give a p-type surface. If this p-type surface (or oxidizing surface, in terms of an n/p ratio) is placed in contact with anions in solution, a greater possibility now exists of electron transfer from the anion to the surface than was the case for the original n-type material. Investigations along these lines with minerals have recently been reported (36). The number of charge carriers in the mineral was obtained from a combination of conductivity measurements (Equation 7) and thermoelectric measurements (Equation 17). From a knowledge of the

band gap of the mineral, obtained from conductivity-temperature plots (Equation 16), the position of the Fermi level was calculated. A good correlation was found between flotation behaviour and the relative n- or p-character of a given mineral. With anion collectors, flotation efficiency increased with increasing p-type behaviour. The surface properties of the mineral were also modified by treatment with oxidizing or reducing agents, a treatment which correlated well with flotation data.

Other techniques are also available to modify the surface electrical properties of minerals. The space-charge region of a semiconductor extends over about 1 micron. Now the diffusion coefficients of some elements, even at room temperature, are sufficiently high that diffusion over a few hundred Angstrom units can occur quite rapidly. If the diffusing species is an acceptor diffusing into an n-type surface, it could change the surface properties by the formation of acceptor levels in the surface region. Thus, the well-known activation of sphalerite (n-type semiconductor) by copper ions for flotation by xanthate (37) may be at least partially explained by the copper ions acting as acceptor centres in the sphalerite surface. A further technique to modify the surface is to use gamma radiation that increases the number of free electrons in the surface region of the semiconductor (i.e., makes it more n-type). This treatment, by the oxidation/reduction analogy, should favour the adsorption of cations over anions. Preliminary work using low radiation doses (few hundred rads) supports this hypothesis (36). Since copious amounts of long-lived fission products from nuclear reactors are readily and cheaply available, the preliminary irradiation treatment of crushed minerals, or in-situ irradiation of flotation systems, appears to have a promising future.

Another area in which the application of semiconductor principles to practical systems would appear to be appropriate is that of electrostatic separation (38). Here, mineral particles are in contact with each other and with metal electrodes. The rectifying properties of the various contacts, the junction capacities involved, and the conductivities of the particles, are

all properties that are related to the Fermi level and subject to modification by suitable pretreatment, temperature, etc.

It should be noted that semiconductor physics may help to explain the fundamental structural properties and the mechanical behaviour of minerals. This type of investigation usually requires a multi-disciplinary approach by solid-state physicists, mineralogists, crystallographers, and chemists. An example of this type of combined research is the work of Keys et al. (39) on iron-bearing zinc sulphide. A possible multi-disciplinary effort appears reasonable from the work of Nickel (40), who points out that the structural difference in pyrite and marcasite (both FeS_2) only shows in the lattice spacing of the second nearest neighbours of marcasite, in which the iron-iron and sulphur-sulphur spacing is closer than the second nearest neighbours of pyrite. The intrinsic band-gap energy of pyrite is 1.1 eV, whereas marcasite has an intrinsic band-gap energy of 0.46 eV (see Appendices 1 and 2). This means that marcasite has a conductivity that is 12 times greater than the conductivity of pyrite. As the density of these two materials is approximately the same, it appears that the higher conductivity of marcasite compared to pyrite may be due to the difference in the bonding energies of the second nearest neighbours of these two minerals. Hulliger and Mooser (41) describe some of the theoretical relationships between the structural bonding and the semiconductor band theory of pyrite and marcasite.

REFERENCES

1. Harvey, D. R., Econ. Geol., 23, 778 (1928).
2. Lawver, J. E., Mines Magazine, 50, 20 (1960).
3. Beam, W.R., "Electronics of Solids" (McGraw-Hill, New York, 1965).
4. Spenke, E., "Electronic Semiconductors" (McGraw-Hill, New York, 1958).
5. Kittel, C., "Introduction to Solid State Physics", 2nd ed. (John Wiley and Sons, New York, 1956).
6. Putley, E. H., "The Hall Effect and Related Phenomena" (Butterworths, London, 1960).
7. Many, A., Goldstein, Y. and Grover, N. B., "Semiconductor Surfaces" (John Wiley and Sons, New York, 1965).
8. Bardeen, J., Phys. Rev., 71, 717 (1947).
9. Garrett, C. G. B. and Brattain, W. H., Phys. Rev., 99, 376 (1955).
10. Green, M., Sci. Prog., 55, 421 (1967).
11. Brown, W. L., Phys. Rev., 91, 518 (1953).
12. Brattain, W. H. and Garrett, C. G. B., Bell System Tech. J. 35, 1019 (1956).
13. Montgomery, H. C. and Brown, W. L., Phys. Rev., 103, 865 (1965).
14. Moss, T. S., "Optical Properties of Semi-Conductors" (Butterworths, London, 1959).
15. Henisch, H. K., "Rectifying Semiconductor Contacts" (Oxford University Press, London, 1957).
16. Dauphinee, T. M. and Mooser, E., Rev. Sci. Instr., 26, 660 (1955).
17. van der Pauw, L. J., Philips Res. Repts., 13, 1 (1958).
18. Fischer, G., Greig, D. and Mooser, E., Rev. Sci. Instr., 32, 842 (1961).
19. Baleshta, T. M. and Keys, J. D., Amer. J. Phys., 36, 23 (1968).
20. Scanlon, W. W., "Properties of Elemental and Compound Semiconductors", H. C. Gatos, ed. (Interscience, New York, 1960).

21. Madelung, O., "Physics of the III-V Compounds" (John Wiley and Sons, New York, 1964).

22. Dekker, A. J., "Solid State Physics" (Prentice-Hall, Inc., Englewood Cliffs, N. J., 1957).

23. Herring, C., Phys. Rev., 96, 1163 (1954).

24. Ioffe, A. F., "Semiconductor Thermoelements and Thermoelectric Cooling" (Infosearch, London, 1957).

25. MacDonald, D. K. C., "Thermoelectricity: an introduction to the principles" (John Wiley and Sons, New York, 1962).

26. Baleshta, T. M. and Carson, D. W., J. Sci. Inst., Series 2, 1, 469 (1968).

27. Spitzer, W. G. and Mead, C. A., J. Appl. Phys., 34, 3061 (1963).

28. Gossick, B. R., "Potential Barriers in Semiconductors" (Academic Press, New York, 1964).

29. Mead, C.A., "Solid-State Elect., 9, 1023 (1966).

30. Goodman, A.M., Surface Science, 1, 54 (1963).

32. Dewald, J. F., Bell System Tech. J., 39, 615 (1960).

33. Grahame, D. C., Chem. Rev., 41, 441 (1947).

34. Myamlin, V. A. and Pleskov, Yv. V., "Electrochemistry of Semi-Conductors" (Plenum Press, New York, 1967).

35. Baddour, R. F. and Selvidge, C. W., "Progress in Solid-State Chemistry", H. Reiss, ed. (Pergamon Press, New York, 1967).

36. Plaksin, I. N., Proceedings of the 8th International Mineral Processing Conference, Leningrad (1968). Preprint.

37. Gaudin, A. M., "Flotation", 2nd ed. (McGraw-Hill Book Co., Inc., New York, 1957).

38. Frass, F., Bureau of Mines, Bulletin 603, United States Department of the Interior, Washington, D. C. (1962).

39. Keys, J. D., Horwood, J. L., Baleshta, T. M., Cabri, L. J. and Harris, D. C., Can. Mineral., 9, 453 (1968).

40. Nickel, E. H., Can. Mineral., 9, 311 (1968).

41. Hulliger, F. and Mooser, E., "Progress in Solid State Chemistry", Vol. 2, H. Reiss, ed. (Pergamon Press, New York, 1965), p. 330.

- - -

APPENDIX 1

Band-Gap Energies of Mineral-Type Semiconductors (Sulphides)

A few sulphide-type mineral semiconductors and their intrinsic band-gap energies (where known) are listed in Table 1. Germanium and silicon band-gap energies are also included in this table, for the purpose of comparison of natural material with synthetic material.

TABLE 1

Band-Gap Energies of Mineral-Type Semiconductors (Sulphides)

Mineral	Chemical Composition	Band-Gap Energy eV
Arsenopyrite	FeAsS	0.16
Bornite	Cu_5FeS_4	0.82
Chalcopyrite	$CuFeS_2$	0.33
Digenite	$Cu_{1.8}S$	-
Galena	PbS	0.38
Marcasite	FeS_2	0.46
Pyrite	FeS_2	1.1
Pyrrhotite	Fe_7S_8	-
Zinc Sulphide	ZnS	3.8
Germanium	Ge	0.75
Silicon	Si	1.2

- - - -

APPENDIX 2

Typical Transport-Measurement Data on Mineral-Type Semiconductors (Sulphides)

The more important transport-measurement data of the minerals listed in Appendix 1 are shown in graphical form (Figures 19 to 37) in this appendix. Where indicated, the conductivity (or resistivity) curves show the effect of the intrinsic band-gap regions of some of the minerals. Otherwise, the conductivity (or resistivity) curves represent a majority of the product of the impurity-charge carriers and their mobility.

(Figures 19-37 follow, on pages 42-60.)

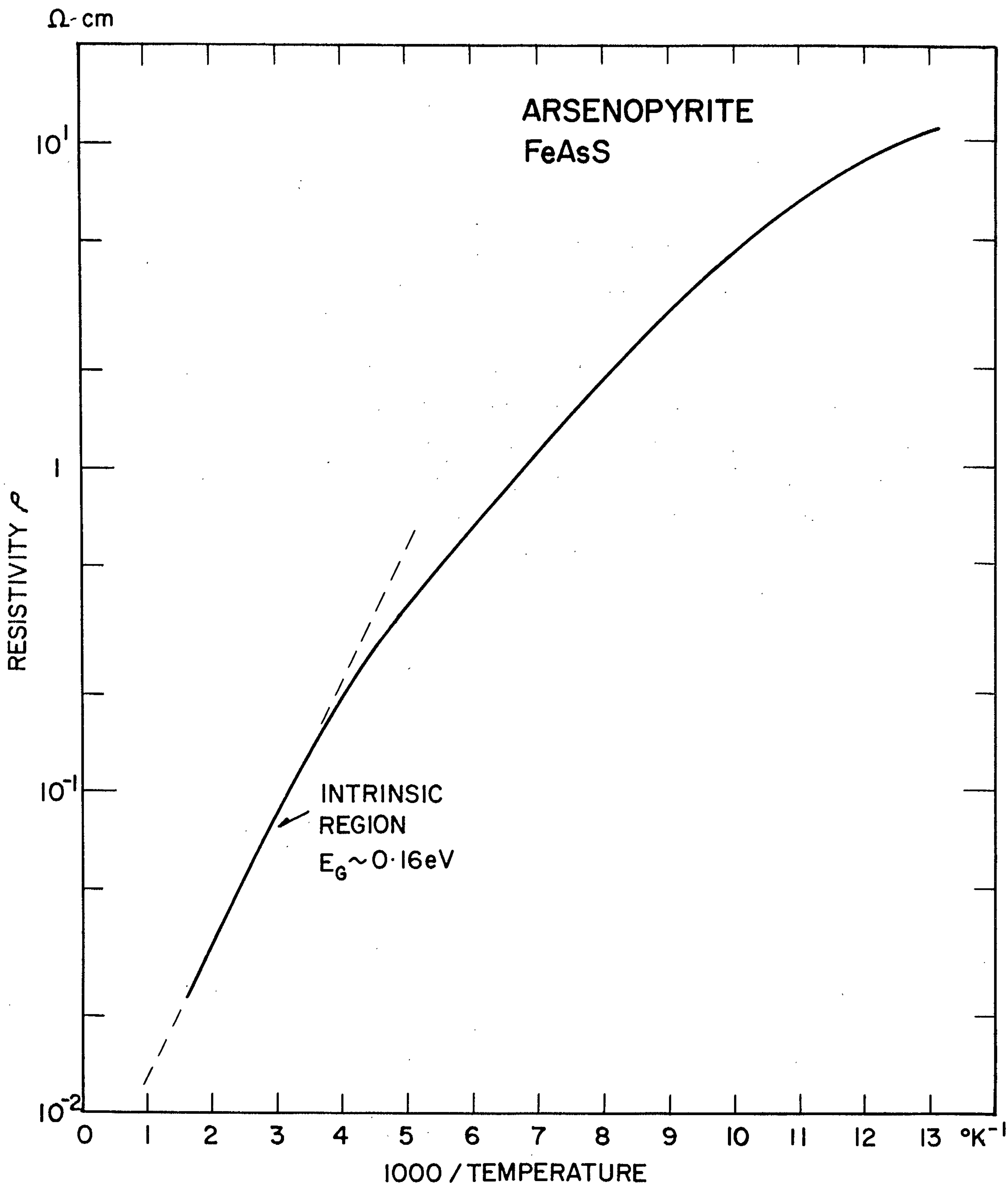

FIGURE 19. Resistivity versus reciprocal temperature of n-type arsenopyrite.

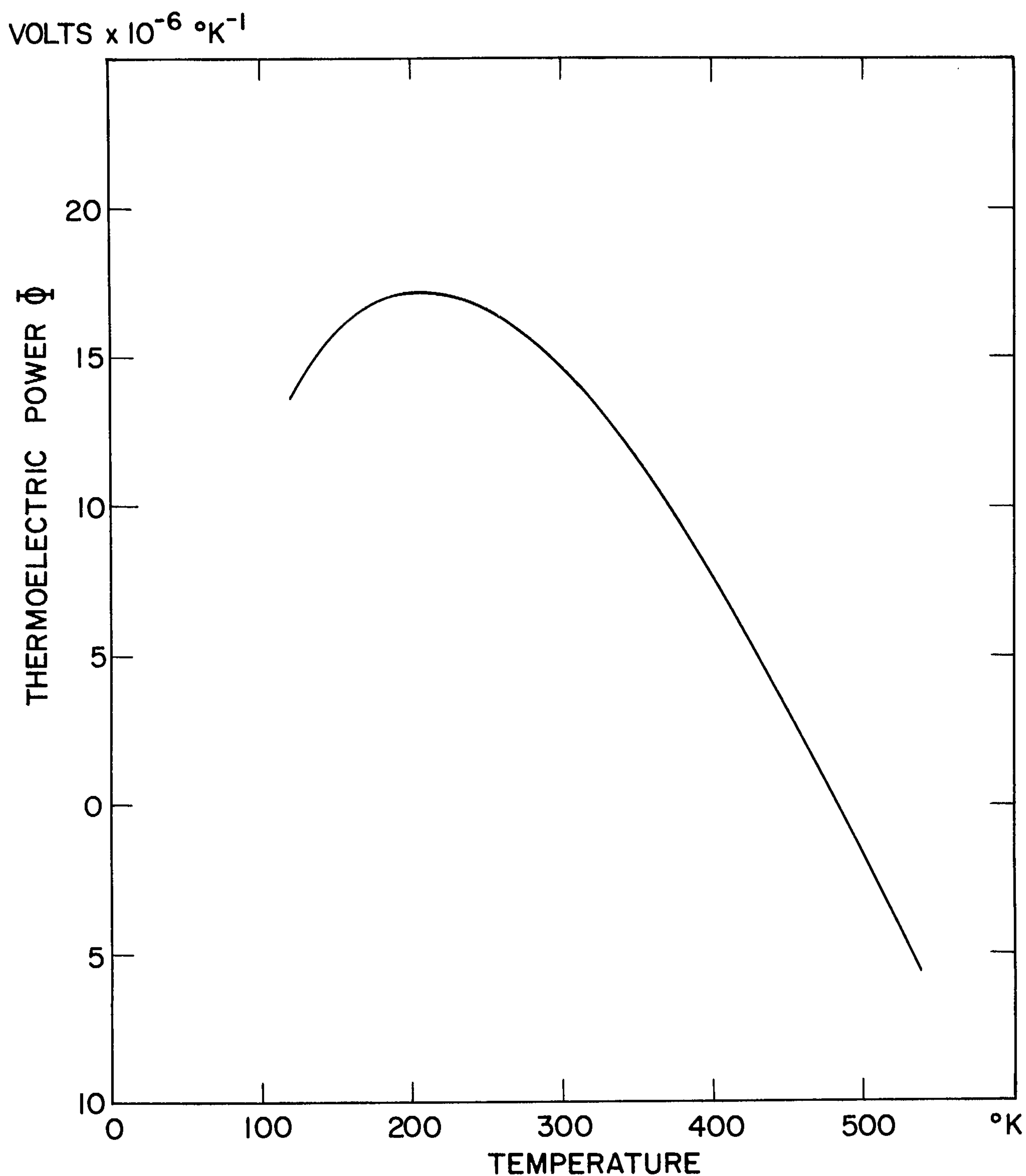

FIGURE 20. Thermoelectric power versus temperature of the arsenopyrite sample in Figure 19.

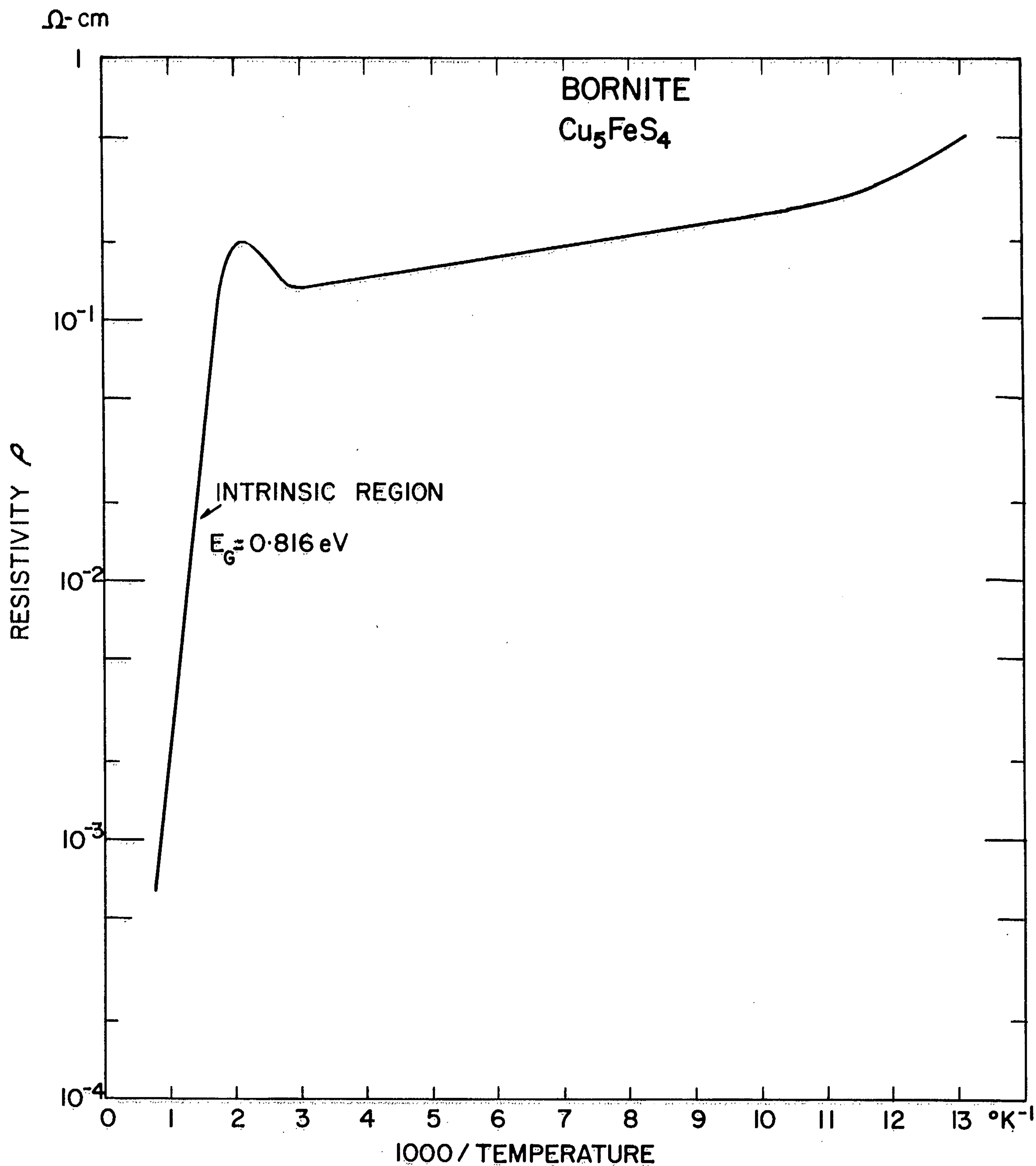

FIGURE 21. Resistivity versus reciprocal temperature of p-type bornite.

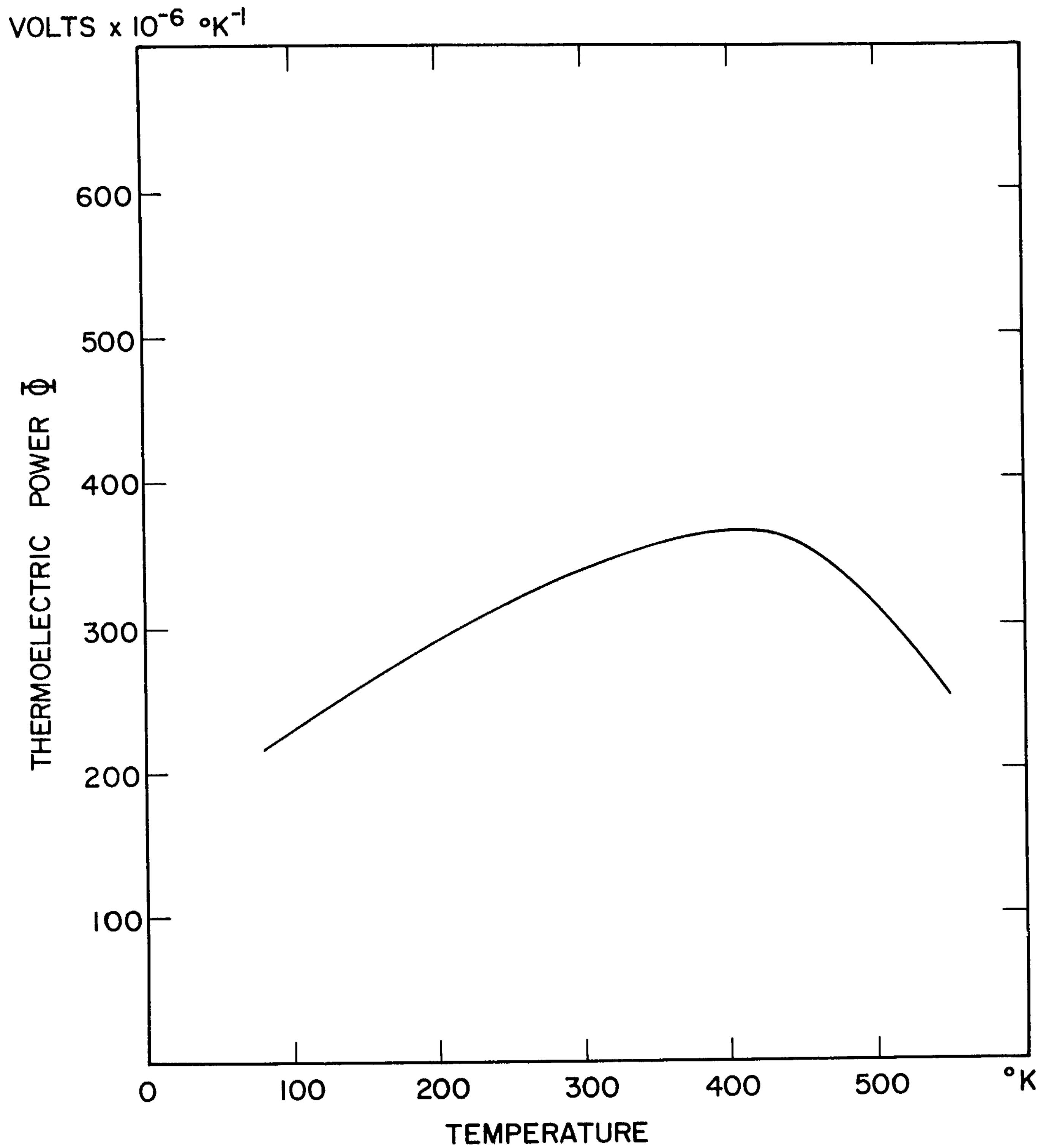

FIGURE 22. Thermoelectric power versus reciprocal temperature of the bornite sample in Figure 21.

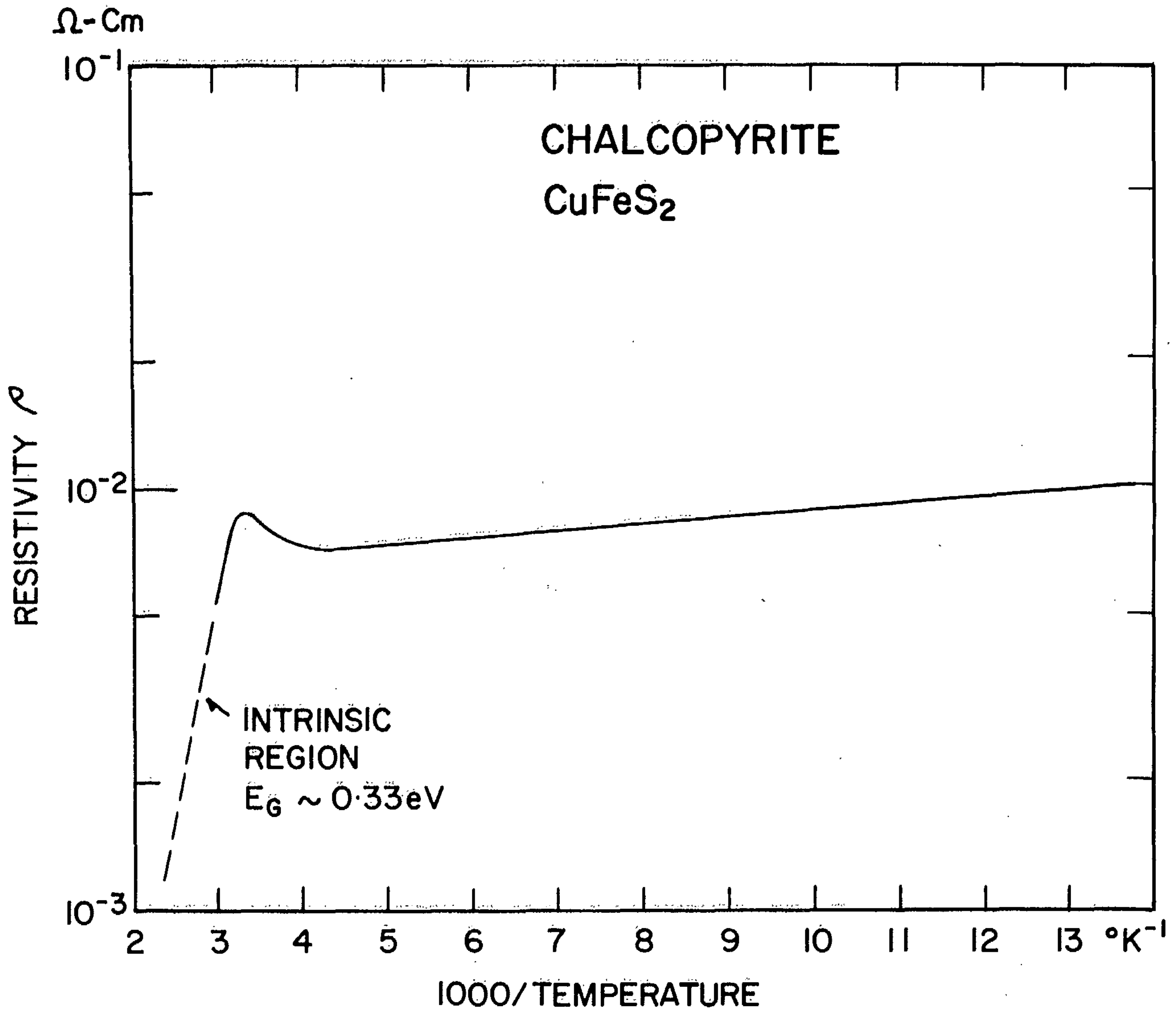

FIGURE 23. Resistivity versus reciprocal temperature of n-type chalcopyrite.

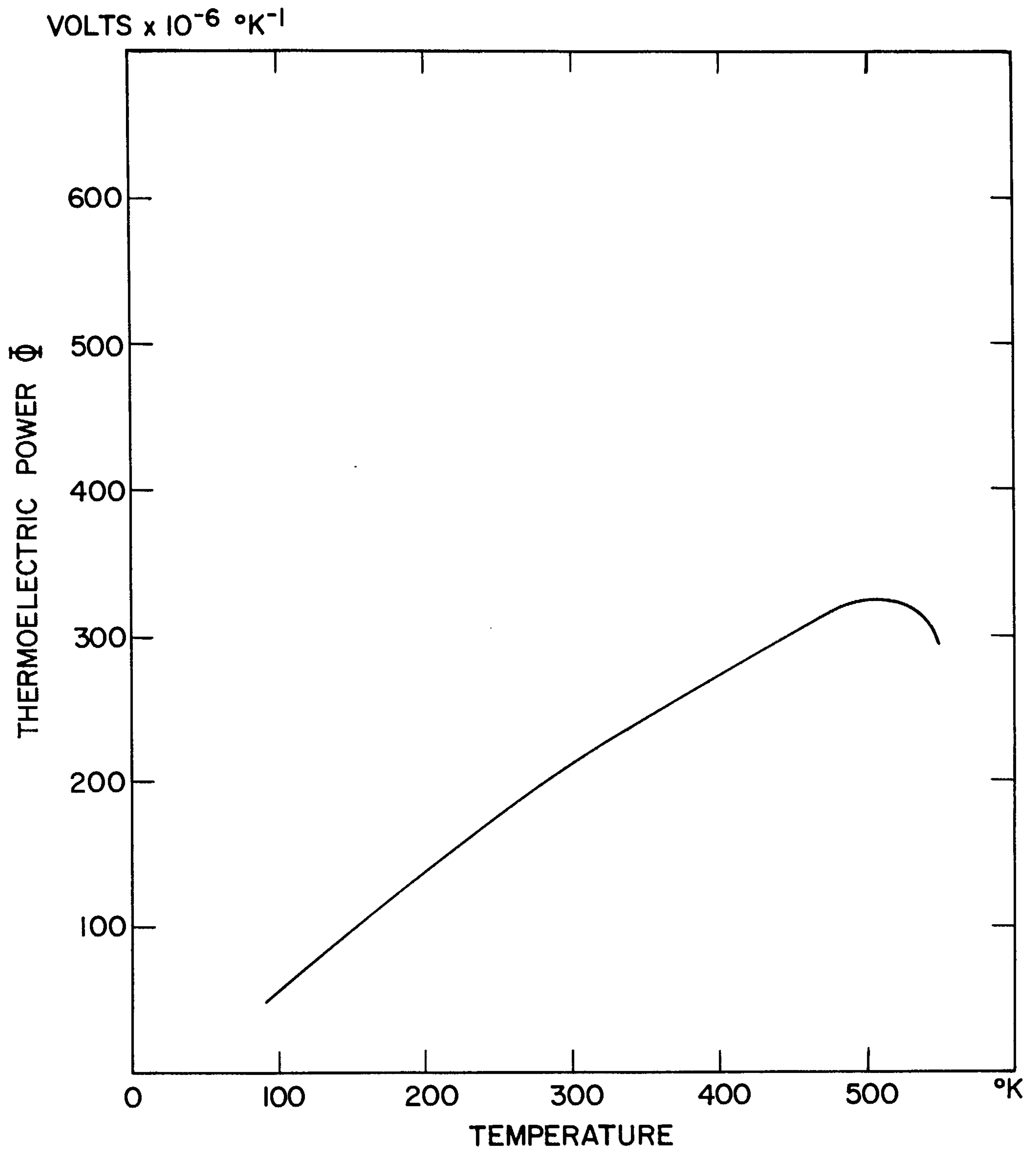

FIGURE 24. Thermoelectric power versus temperature of the chalcopyrite sample in Figure 23.

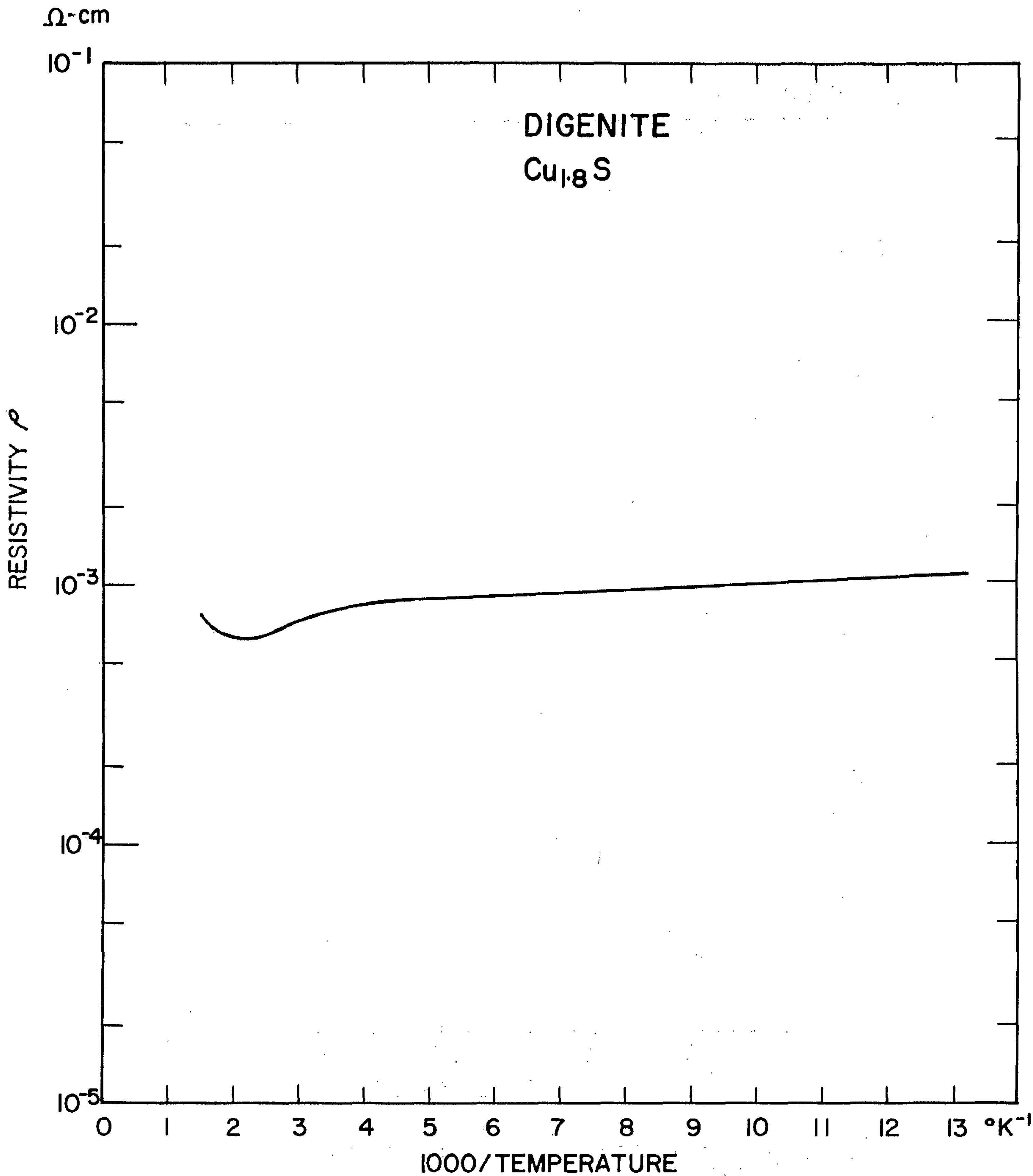

FIGURE 25. Resistivity versus reciprocal temperature of p-type digenite.

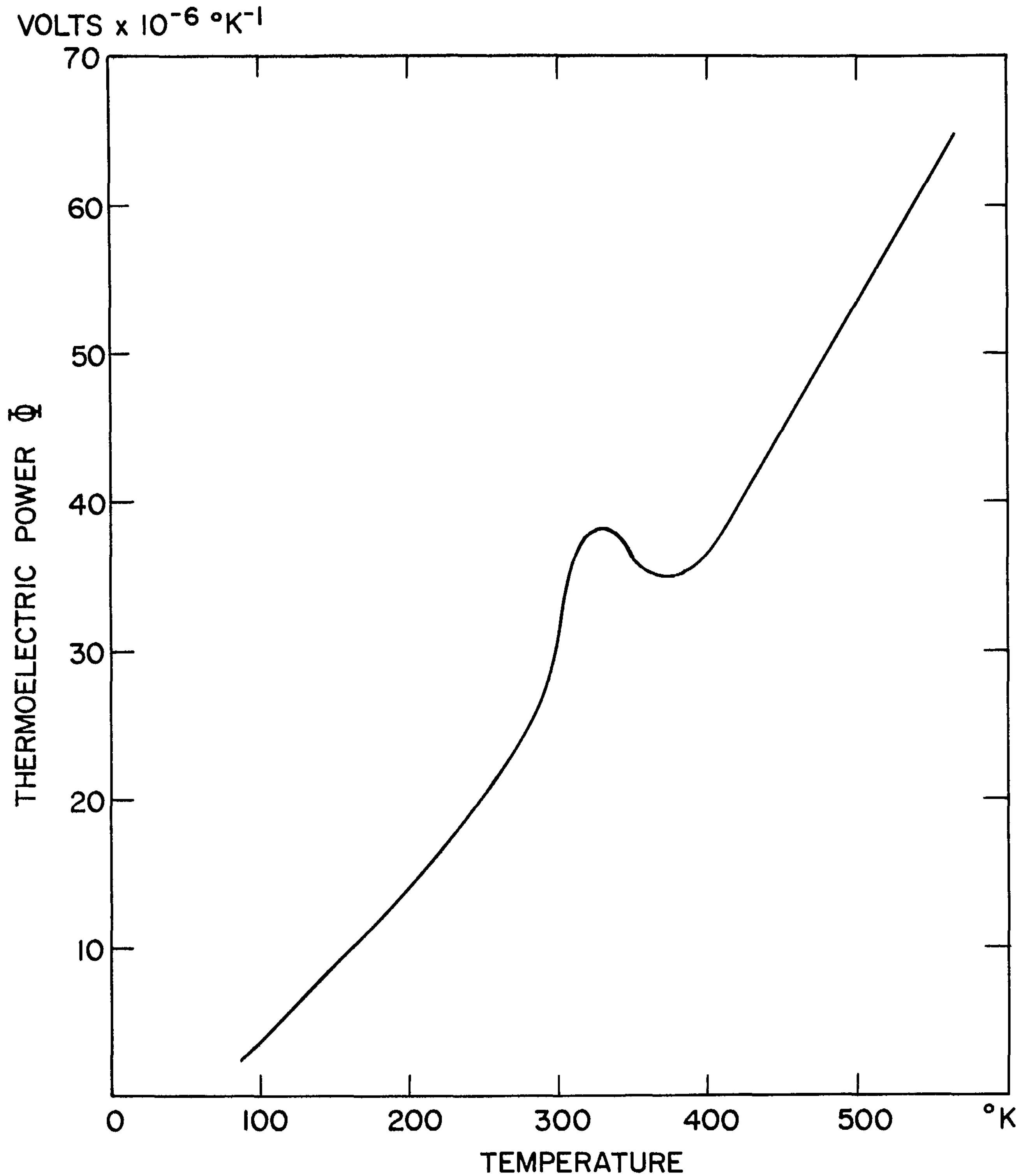

FIGURE 26. Thermoelectric power versus temperature of the digenite sample in Figure 25.

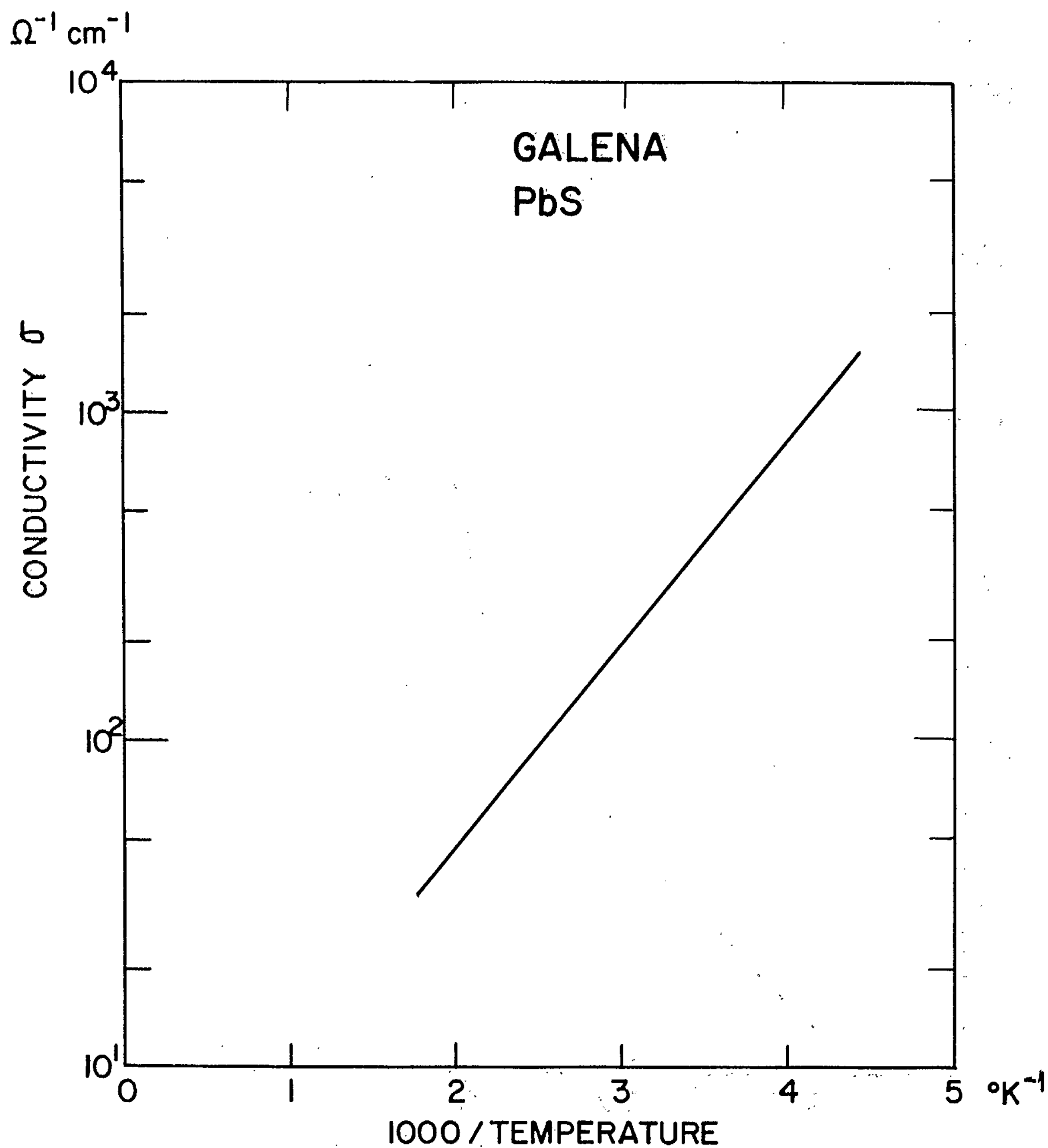

FIGURE 27. Conductivity versus reciprocal temperature of synthetic galena, p-type. Activation energy 0·12 eV.

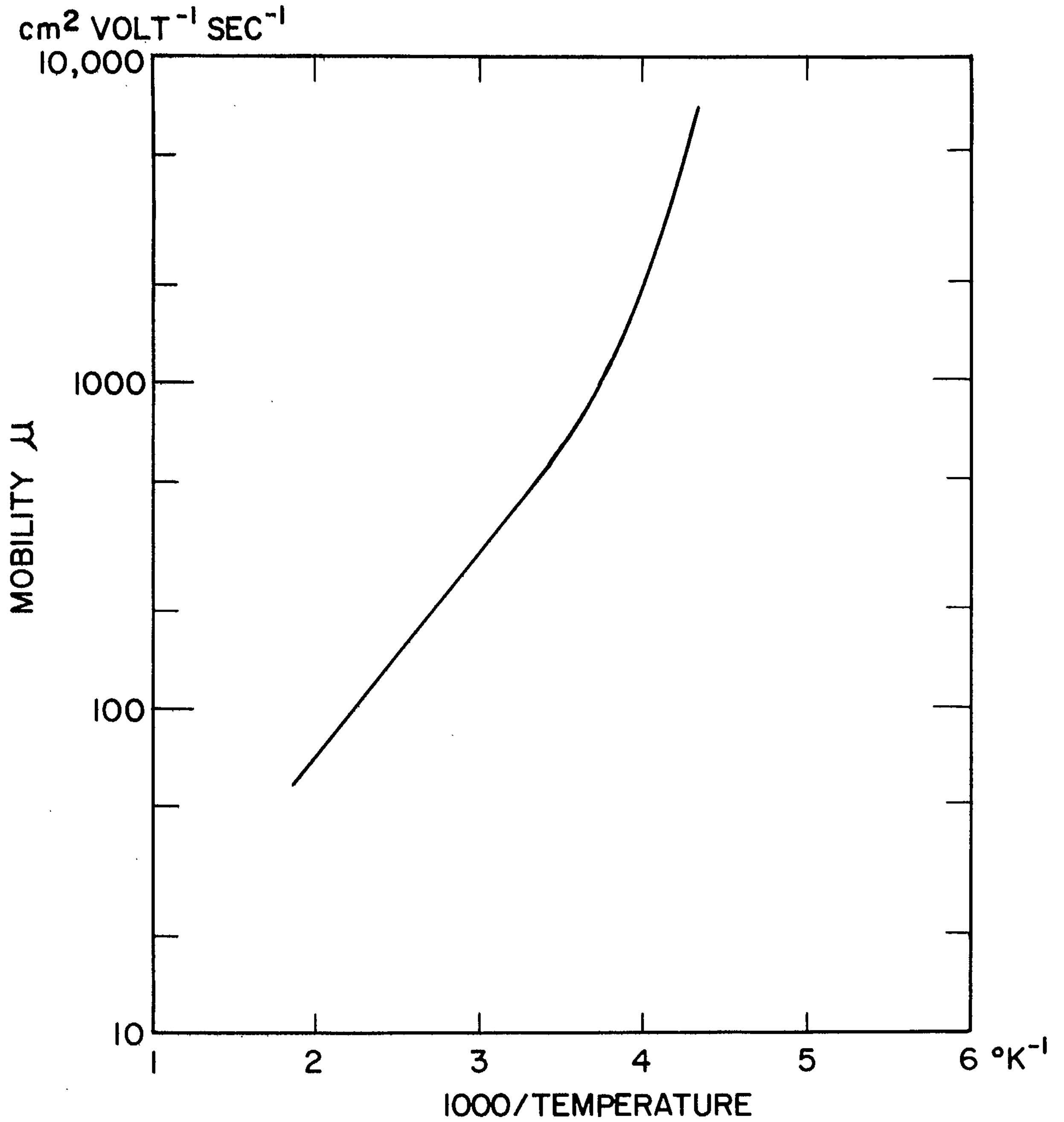

FIGURE 28. Hole mobility versus reciprocal temperature of the galena sample in Figure 27.

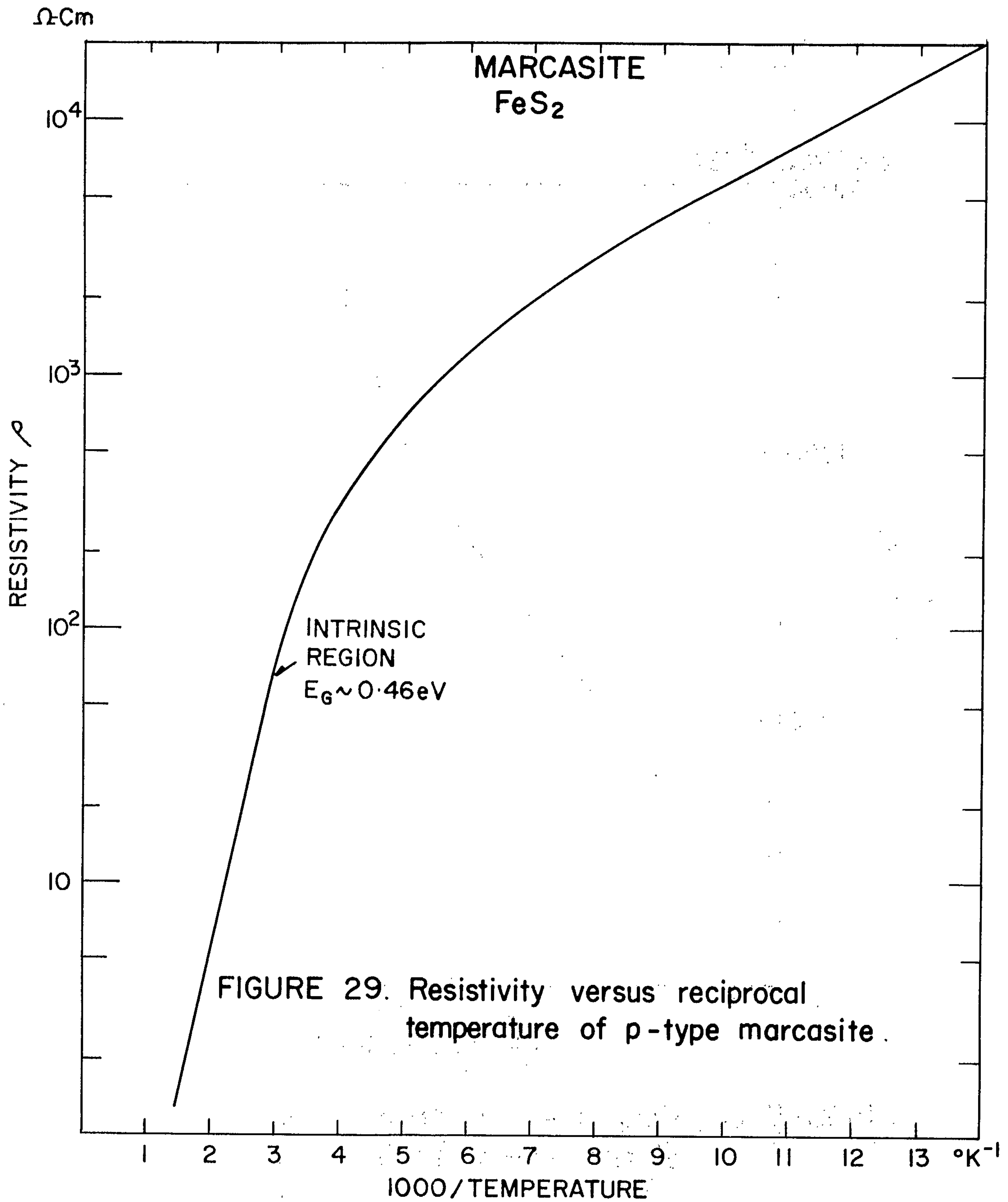

FIGURE 29. Resistivity versus reciprocal temperature of p-type marcasite.

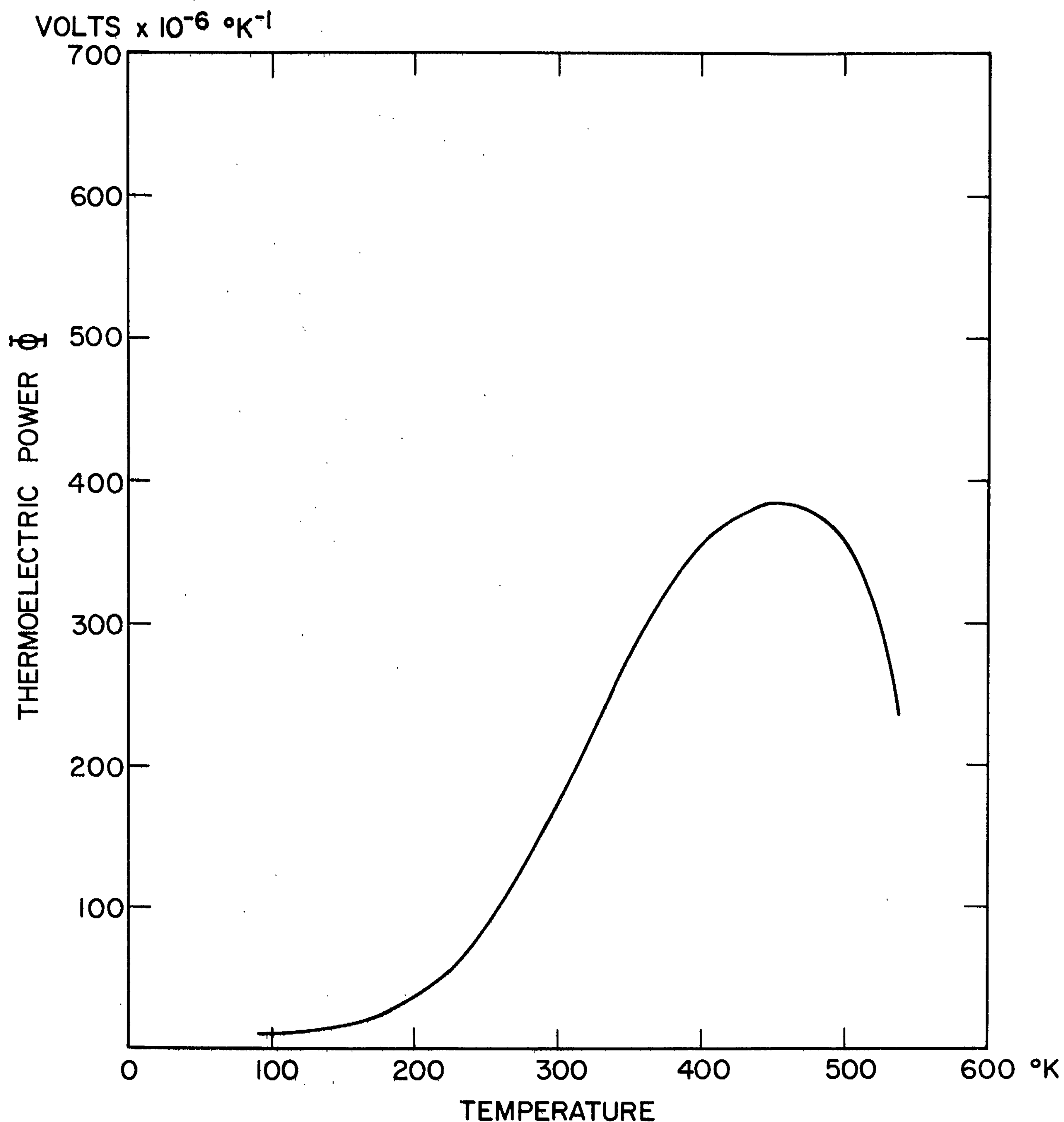

FIGURE 30. Thermoelectric power versus temperature of the marcasite sample in Figure 29.

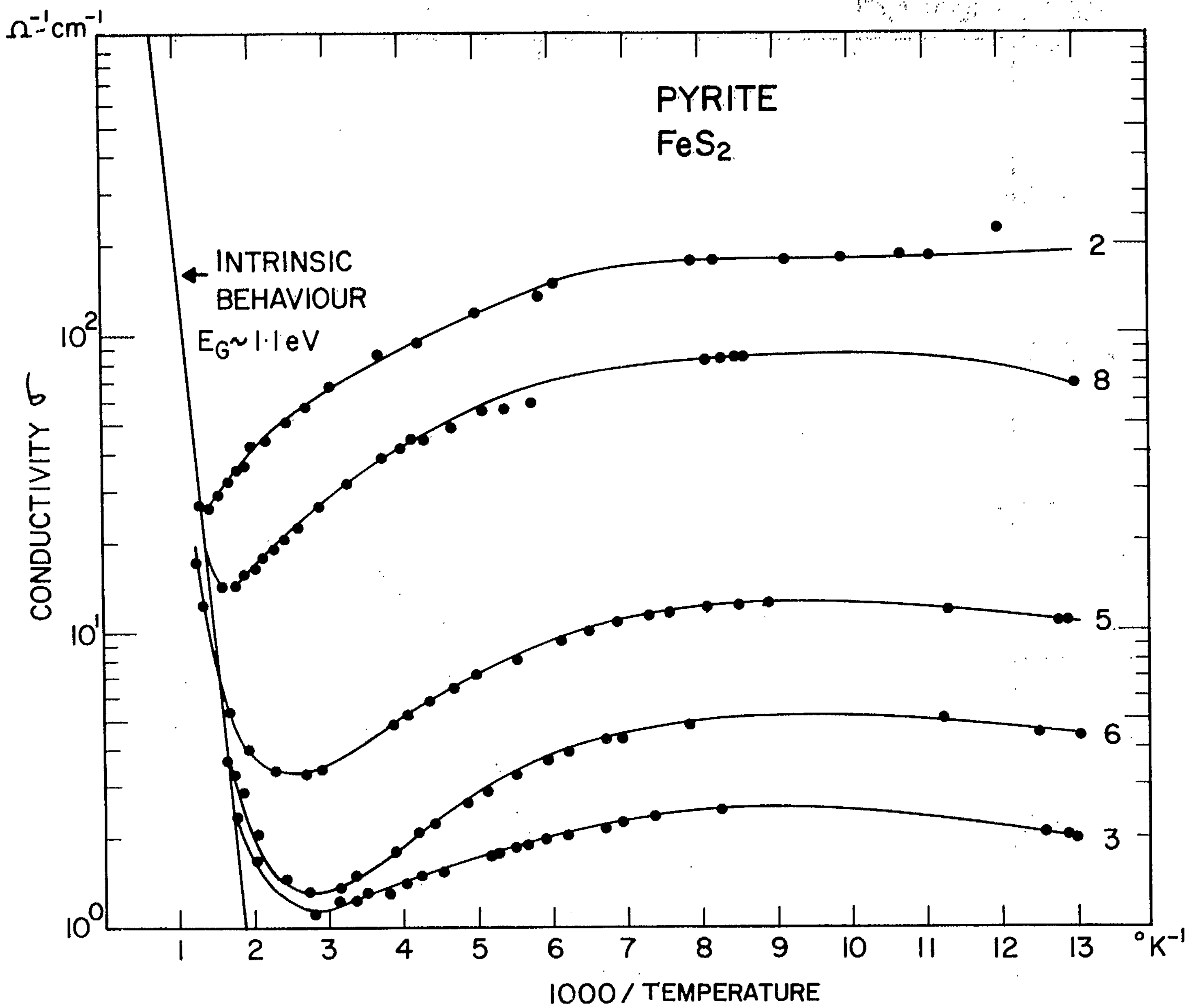

FIGURE 31. Conductivity versus reciprocal temperature of a variety of n-type pyrite samples.

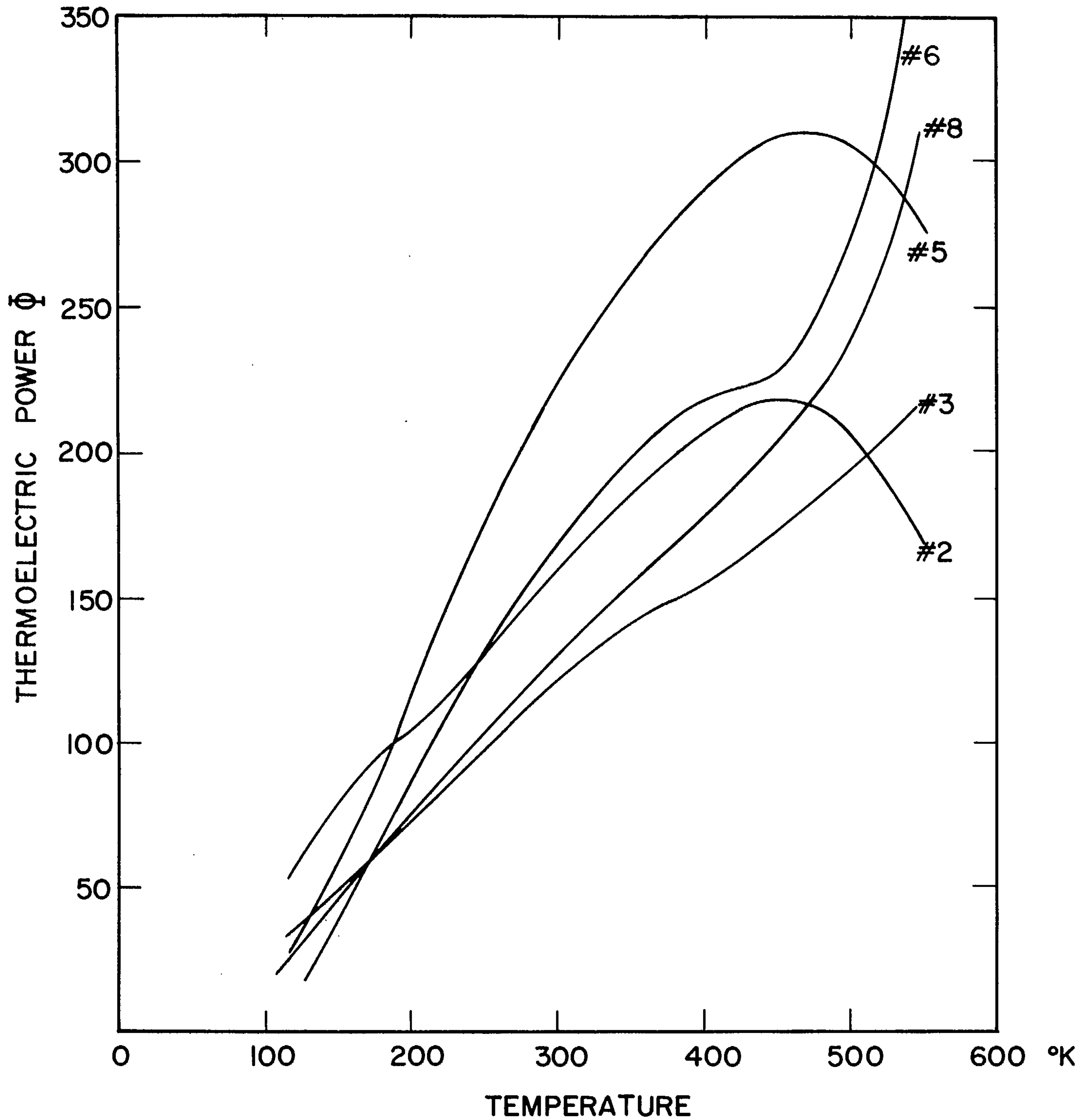

FIGURE 32. Thermoelectric power versus temperature of the n-type pyrite samples in Figure 31.

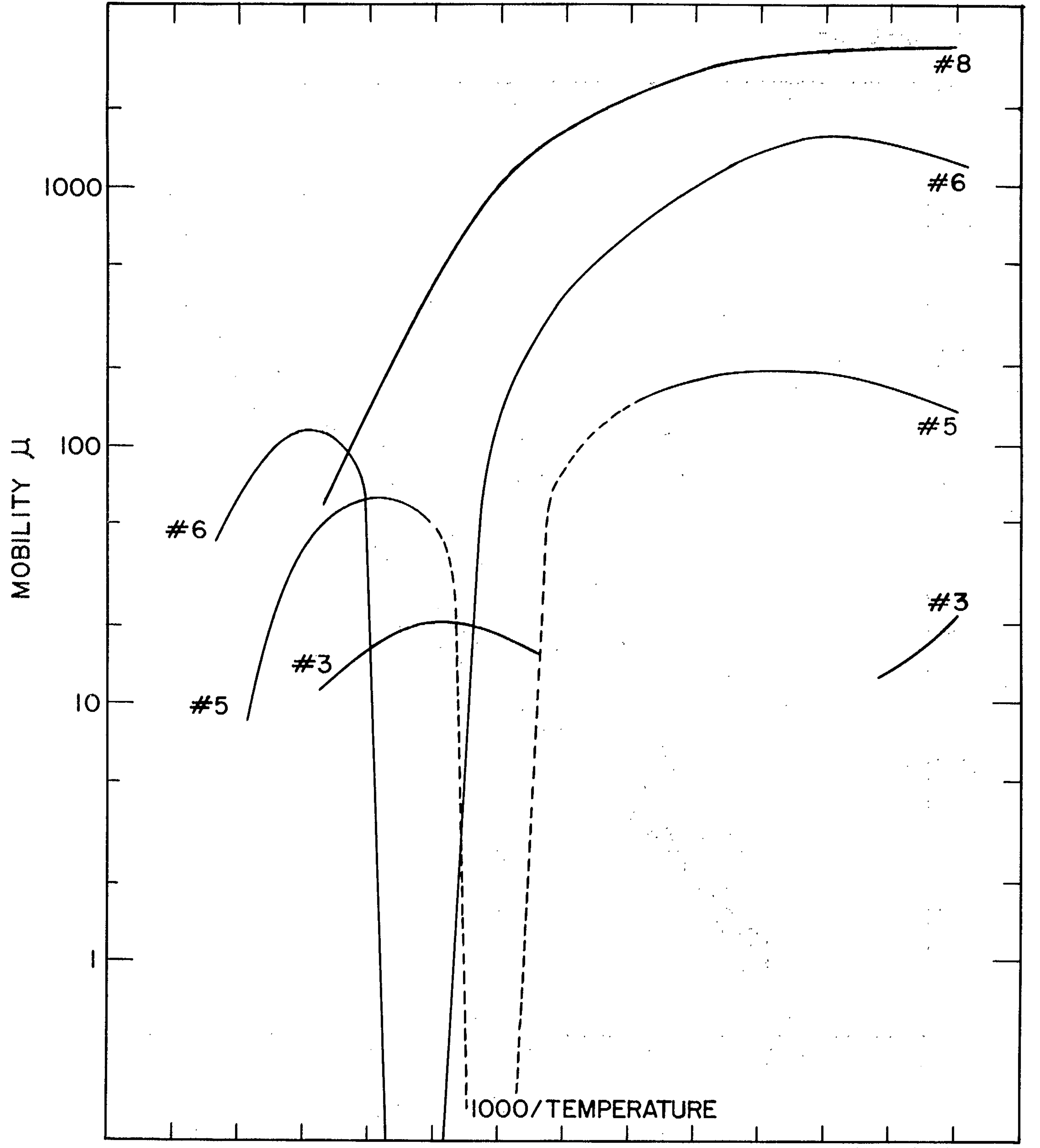

FIGURE 33. Mobility versus reciprocal temperature of the pyrite samples in Figure 31.

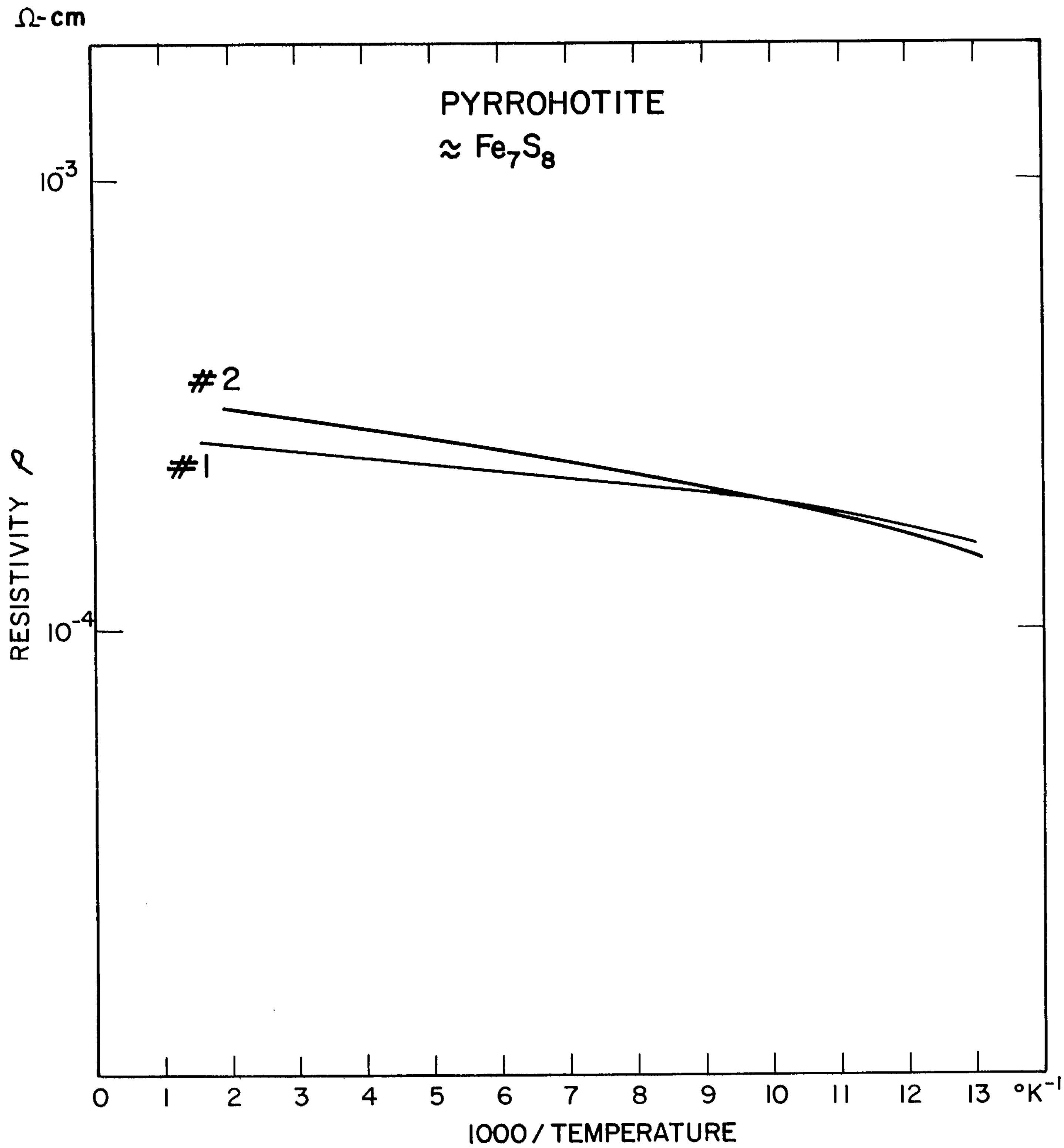

FIGURE 34. Resistivity versus reciprocal temperature of two p-type pyrrhotite samples.

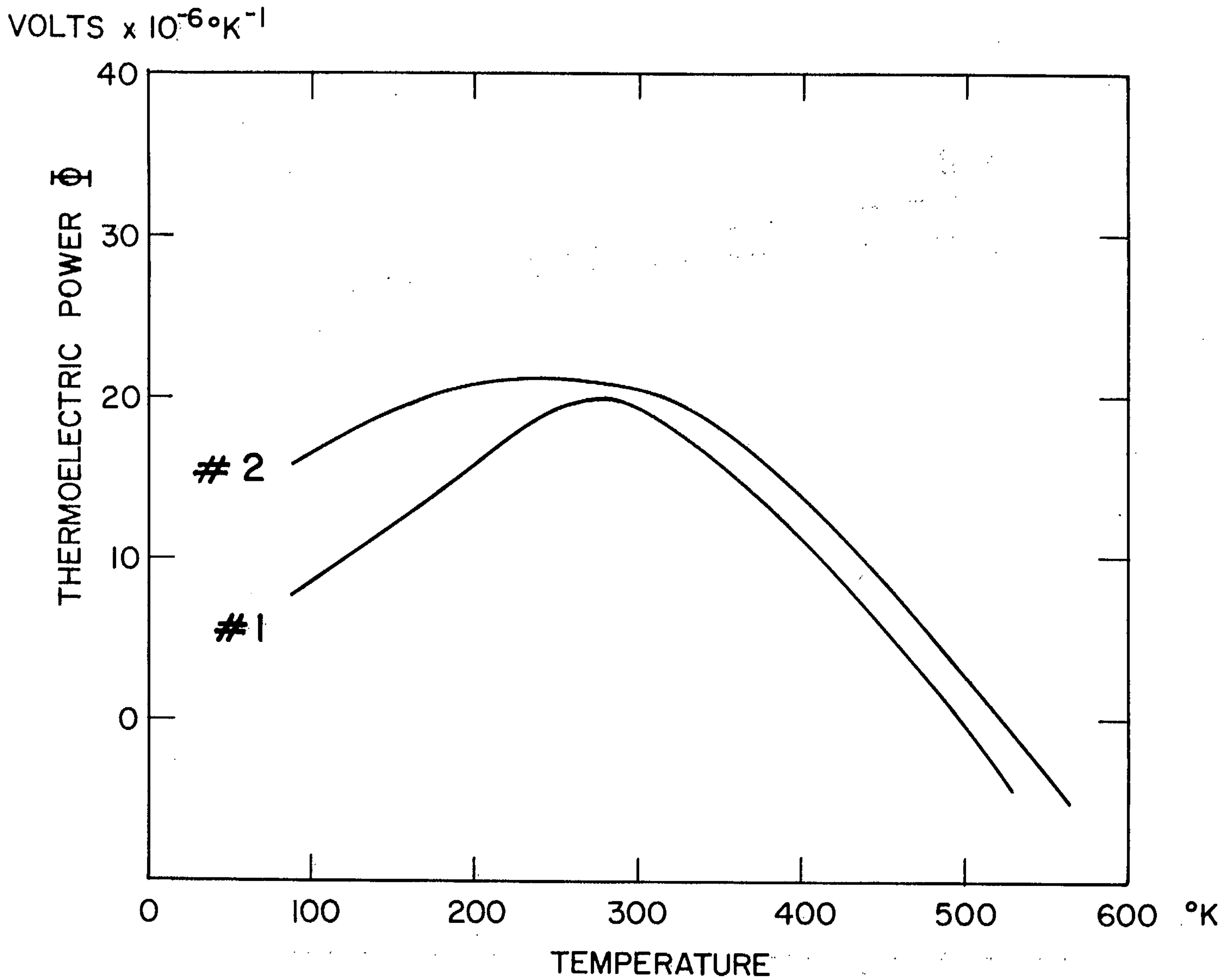

FIGURE 35. Thermoelectric power versus temperature of the pyrrhotite samples in Figure 34.

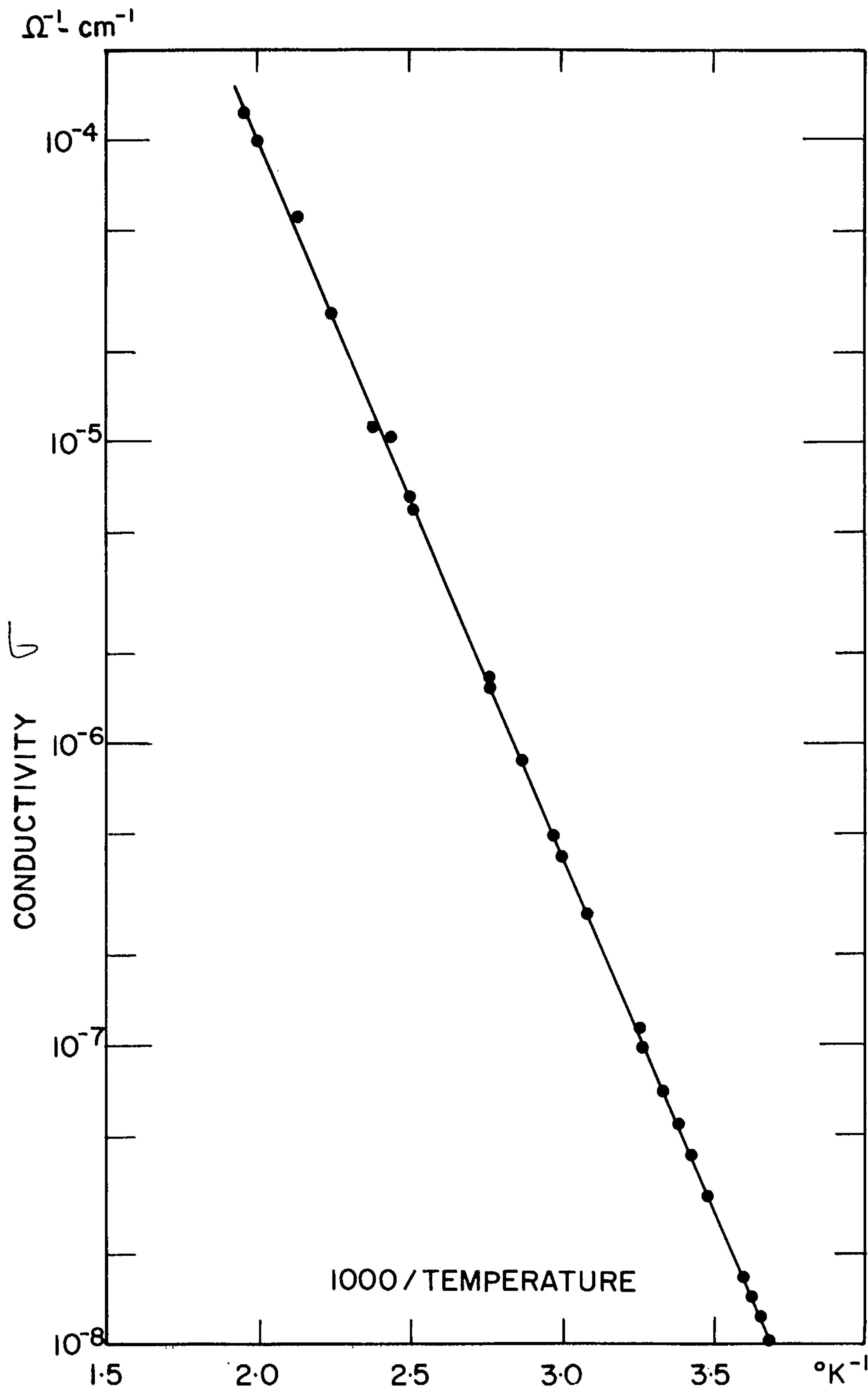

FIGURE 36. Conductivity versus reciprocal temperature of zinc sulphide - 16 wt % iron doped (p - type).

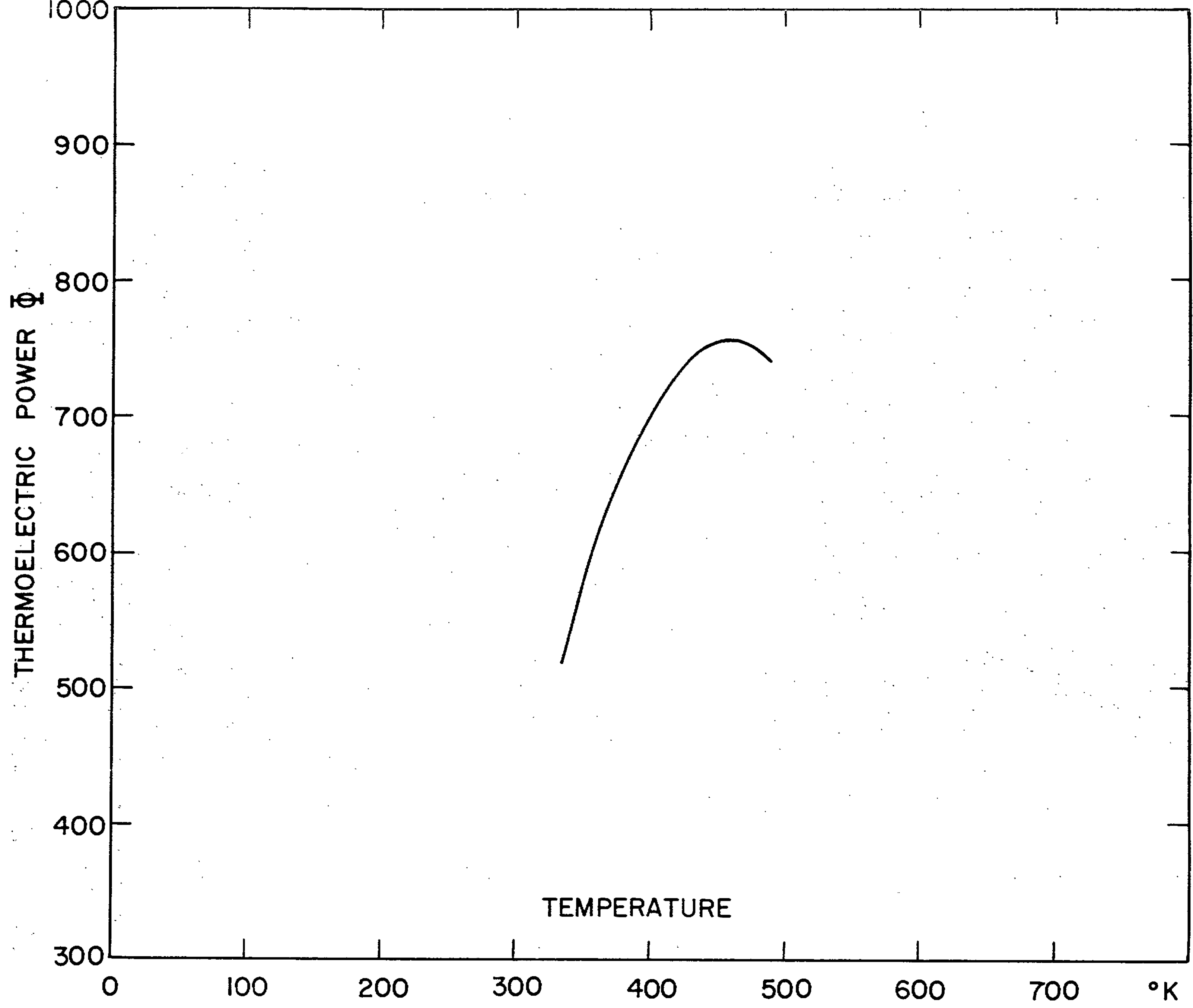

FIGURE 37. Thermoelectric power versus temperature of the zinc sulphide sample in Figure 36.